Deep Sea Research Part I: Oceanographic Research Papers
March 2023, Volume 193 Pages 103956 (12p.)
https://doi.org/10.1016/j.dsr.2022.103956
https://archimer.ifremer.fr/doc/00812/92429/

Update of the PERISCOP system for isobaric sampling of deep-sea fauna

Shillito B. [1,*], Amand L. [1,2], Hamel G. [2]

[1] Laboratoire de Biologie des Organismes et Ecosystèmes Aquatiques (BOREA), MNHN, CNRS-8067, IRD-207, Sorbonne Université, UCN, UA, France
[2] Institut de Minéralogie, de Physique des Matériaux et de Cosmochimie (IMPMC), Sorbonne Université, CNRS, MNHN, IRD, 4 Place Jussieu, 75252 Paris Cedex 05, France

* Corresponding author : B. Shillito, email address : Bruce.Shillito@sorbonne-universite.fr

Abstract :

We here present an update of the PERISCOP pressurised recovery device (PRD), which has allowed the recovery of live deep-sea fauna, following active sampling by manned or remotely-operated submersibles. It was designed in 2006, has since been deployed almost a hundred times (93), and its operation has now become almost routine. Various hydrothermal vent megafaunal organisms (shrimp, crabs, annelids, mussels, fish,..) were successfully targeted and recovered, allowing access to samples in excellent physiological condition. Gradually, the system was modified, aiming at improved reliability, depth of operation, and simplicity of use, especially regarding its compensator, i.e. the system that compensates for pressure loss experienced during ascent through the water column. Two types of compensators are presented, called “active” and “passive” (with so-called “water-filled” or “oil-filled” modes regarding the latter). Their respective uses are reported and discussed here, and while the active system proves more efficient (recovering at minimum pressure in the range 93.8–98.2% of in situ pressure, as opposed to 80.9–86.6% for the water-filled passive system, while no compensation leads to a range of 63.5–73.0%), the simplicity of the passive compensator greatly improves reliability and ease of use and maintenance. Finally, the monitoring of pressure and temperature of the PRD and the surrounding water column permits to discuss various technical aspects of pressurised recovery, and to propose further improvements.

Highlights

► The PERISCOP pressurised recovery device (PRD) aims at recovering live deep-sea fauna, following active sampling by manned or remotely-operated submersibles. It has been deployed almost a hundred times (93) since its initial design in 2006, at depths ranging from 800 to 3600 m. Its operation has now become almost routine, with the successful recovery of various hydrothermal vent megafaunal organisms (shrimp, crabs, annelids, mussels, fish,..), in excellent physiological condition. Several improvements of the system are presented in terms of reliability, depth of deployment, simplicity of use, and a focus is made on its compensator, i.e. the system that compensates for pressure loss experienced during ascent through the water column. Two types of compensators are presented, called “active” and “passive”. Their respective uses are reported and discussed here, and while the active system proves more efficient, the

simplicity of the passive compensator greatly improves reliability and ease of use. Finally, in the light of the field experience acquired with the PERISCOP PRD, various technical aspects of pressurised recovery are discussed, and further improvements are proposed.

Keywords : Isobaric sampling, Hydrostatic pressure, Pressure compensation, Physiology

INTRODUCTION

The deep sea is by far the largest ecosystem on the planet, but it remains the least explored and understood (Ramirez-Llodra et al, 2010, Fang et al, 2010), especially regarding the ecology and biology of the organisms inhabiting this environment. One evidence is emerging though: the deep-sea biome is threatened by climate change and other anthropogenic stressors (Ramirez-Llodra et al, 2011, Sweetman et al, 2017). Providing significant advances in fundamental knowledge on the ecology, biology, and physiology of deep-sea organisms is therefore an urgent matter, but this goal is challenged by the difficulties in accessing their habitat. Accessing deep-sea habitats often requires distant and costly high-sea expeditions, and the use of equipments specifically adapted to the environmental parameters prevailing at depth. Among those parameters, the major obstacles to investigations are low temperatures and high hydrostatic pressures, especially for physiological studies, as witnessed by the apparent trauma inflicted to deep fauna recovered with neither temperature nor pressure control. As recently reviewed in MacDonald (2021), it is quite clear today that isobaric and isothermal sampling are needed prior to undertaking physiological studies of deep biota.

The PERISCOP pressurised recovery device (PRD) was designed in our laboratory, and first operated at sea in 2006. It aimed at recovering mobile hydrothermal vent fauna in good physiological conditions, from depths as great as 3000 m (Shillito et al, 2008), by maintaining the pressure and temperature prevailing in the environment of these organisms. It has since been operated several times (93), allowing for example the deepest recovery of a live fish (*Pachycara saldanhai*, Shillito et al, 2008), or the first *in vivo* determination of thermal resistance, in the case of the thermophilic vent tubeworm (*Alvinella pompejana*, Ravaux et al, 2013). The PERISCOP was gradually modified, aiming at improved reliability, and simplicity of use. One specific focus was the compensator of the PRD, i.e. the system that compensates for pressure loss experienced during ascent through the water column (Shillito et al, 2008).

We here present an update of the PERISCOP PRD, with improvements based on data and practical experience we acquired at sea. We hope this work provides help to other investigators, in the design and operation of future PRDs.

METHODS

The PERISCOP Pressurised Recovery Device (PRD) (Figure 1)

PERISCOP is a PRD of internal volume of 6.6 L, and is constructed with 316 or APX4 stainless-steel type components (Figure 1). It is also described in Shillito et al (2008), and main modifications are indicated below. Pressure inside the PRD is recorded by an autonomous probe (SP2T 4000, NKE instruments, Hennebont, France), while an optional temperature logger may be inserted inside the PRD (S2T 6000, NKE instruments, Hennebont, France). All the probes were pre-set to record data once every minute throughout each deployment. The PRD's main aperture is a quarter-turn globe-valve allowing a 10 cm diameter free passage, whereas the bulk of the PRD is a cylinder of 10.6 cm internal diameter and 50 cm length. The PRD is enclosed in a rectangular-shaped syntactic foam casing, which contributes to both thermal insulation and floatability. Compared to the first PERISCOP described in Shillito et al (2008), the major modifications consisted in re-designing the collar-shaped clamps that maintained the globe-valve and the sampling cylinder together (see figure 3 in cited reference), in order to obtain a more rigid behaviour under pressure, and to increase its maximum depth of operation from 3000 to more than 3600 m. In order to improve both thermal insulation and floatability, the casing was redesigned with a syntactic foam of lower density (from 0.54 to 0.42, same manufacturer, BMTI Toulon France), and its side dimensions were slightly enlarged (from 32 to 34 cm). As a result, the weight of the entire device is 113 kg, appearing at 36 kg under water (104 kg and 43 kg respectively for the PRD described in Shillito et al , 2008).

The two types of pressure compensators (Figure 1C, 2 and 3)

During ascent through the water column, changes in environmental pressure and temperature can modify the pressure prevailing inside the PRD, because of metal expansion and seal movements, thereby justifying the use of a pressure compensation unit (or so-called compensator). Unlike most other PRDs, our compensators do not rely on pressurized gas, and two systems are presented: one called active, as opposed to the other, named passive. The principles are described in figures 2 and 3 respectively. Briefly, the active compensator requires that a high-pressure reservoir is loaded with seawater at a pressure of about 45-50 MPa before each deployment (on board ship), and that a reference container is closed *in situ* by the submersible's hydraulic arm, just before the PRD begins the ascent to the surface, in addition to closing the PRD's main globe-valve (Figure 2). From then on, the compensator, by means of two differential valves (Tescom, Elk River, Minnesota, USA), compares the pressures prevailing in the reference container and the PRD, and consequently compensates for either pressure loss or gain in the PRD (see Figure 2). It is this active compensator that was first designed and used (Shillito et al, 2008), and major improvements consisted in 1 - integrating the differential valves inside the main container, at atmospheric pressure (they were previously exposed to surrounding pressure, see Figure 2 in Shillito et al, 2008), and 2 - increasing the volume of the reference container, from 90 mL to 300 mL (stainless steel container, HOKE-LAA, Asnières, France). The weight of the active compensator is 27.85 kg.

Alternatively, the passive compensator does not require pre-conditioning prior to each deployment, and the only manipulation required *in situ* is the closing of the main globe-valve of the PRD. Unlike the active system, which integrates off-the-shelf components, this compensator was entirely designed in our laboratory, with the help of computer-assisted design facilities (SolidWorks, Dassault systems, France). Its principle relies on the elasticity of its internal container (of 4 L internal volume, made of Titanium TA6V alloy), and the compressibility of the liquid it contains (either water or oil). This container is stored in an external container (made of 316 stainless steel alloy), and is therefore always surrounded by atmospheric pressure during deployments. Upon mooring at depth, the environmental pressure “loads” the compensator with seawater by pushing a piston (see Figure 3). During recovery (ascent through the water column) this seawater is provided to the PRD as its internal volume expands due to the decreasing surrounding pressure. The weight of the passive compensator is 26.7 kg.

Operation of the PERISCOP PRD by a submersible and associated shuttle device (Figure 4)

The PERISCOP system is attached to a shuttle device, which allows mooring and recovery of various instruments and tools related to the submersible’s activity during scientific dives. The shuttle presented in Figure 4 belongs to the Nautile team (Ifremer’s manned submersible, so-called Human Occupied Vehicle, or H.O.V.), however the PERISCOP has also been successfully used with two other shuttle devices belonging to the Victor 6000 team (Ifremer’s Remotely Operated Vehicle, or R.O.V., see Shillito et al, 2008). As described in Shillito et al , 2008, the PERISCOP system allows active sampling of fauna by means of a deep submersible, i.e. it allows choosing for samples, as opposed to most other PRDs which rely on attraction of fauna to bait. In order to track the pressure history of samples with respect to the recovery sequence, an additional autonomous probe (SP2T 4000, NKE Instruments, Hennebont, France) is mounted on the shuttle, and records the temperature and pressure of the surrounding water column.

In situ sampling process (Figure 5)

As previously described (Shillito et al, 2008), the sampling cell is made from PVC and transparent Polycarbonate. It mainly consists of two interlocked cylinders, an outer cylinder connecting to the submersible’s suction device, and an inner cylinder for confinement of fauna, with an internal diameter of 95 mm and length of 350 mm. Fauna are sampled using the suction power of the submersible, through a 50 mm diameter flexible nozzle. The suction device of the submersible is connected to the sampling cell *in situ* immediately prior to sampling, and disconnected afterwards. Once this has been done, the submersible separates the two cylinders composing the sampling cell. The inner cylinder contains the samples, and will be stored further inside the PRD, before allowing the shuttle to ascend towards the surface.

In the case of sessile fauna, which can be sampled directly with the submersible's hydraulic claw, another sampling cell made of 316 stainless steel was designed (and named "Croco"), which allows direct positioning inside the PRD once the sampling cell is closed (see Figure 6 E-F, and Ravaux et al, 2013).

RESULTS

Overview

Overall, the PERISCOP PRD was operated 93 times, at East Pacific Rise (EPR) vents (14 deployments), Mid Atlantic Ridge (MAR) vents (67 deployments), and in the Mediterranean Sea (a few nautical miles off Toulon, on the French coast, 12 technical deployments), at depths ranging from 750 to 3650 m. 49 of these deployments were achieved with the manned submersible Nautile, and 44 with the R.O.V. Victor 6000. Various hydrothermal vent organisms were sampled and further studied *in vivo* on board the oceanographic ship, using dedicated pressure aquaria (Shillito et al, 2014): alvinellid tubeworm colonies (*Alvinella pompejana* and *Alvinella caudata*) and associated fauna (not shown, see Ravaux et al 2013, Papot et al, 2017), bythograeid crabs *Bythograea thermhydron* (not shown), vent mussels *Bathymodiolus azoricus* (Figure 6 E-F, see also Szafranski et al, 2015), *Bathymodiolus puteoserpentis* and associated fauna (not shown, see Duperron et al, 2016, Piquet et al 2019, 2020). MAR hydrothermal vent shrimps *Rimicaris exoculata*, *Rimicaris chacei*, and *Mirocaris fortunata,* were the main targets, totalising 51 deployments (see Figure 5A, and Figure 6 A-B, see also Auguste et al 2016, Methou et al 2019, Le Bloa et al, 2020, Ravaux et al 2009, 2019, 2021, for recent biological studies). Finally, 3 zoarcid fishes, 1 *Thermarces Cerberus* (not shown), and 2 *Pachycara saldanhai* (Figure 6 C-D, see also Shillito et al, 2008) were sampled and recovered in good physiological condition, as witnessed by their behavioural activity.

Regarding the use of different pressure compensation systems, 48 deployments used the active compensator, 32 used the passive compensator, and 8 deployments occurred without any compensator. Finally, 5 deployments did not retain pressure, resulting either from a deliberate choice, or from important leakage during recovery.

In terms of reliability, all 8 deployments without compensation behaved as expected (100 % reliability), i.e. recovering at a minimum of 60% of *in situ* pressure, with only one minor leak detected (EssNaut 2021 # P3 deployment). For the 32 deployments using the passive compensator, 30 behaved as expected, i.e. recovering at pressures above 80 % of *in situ* values (~ 94 % reliability), despite minor leaks detected in two of these deployments (see Table S2). The two remaining deployments experienced a failure of the autonomous pressure probe (no data), or a leak during ascent resulting in 71 % retention of *in situ* pressure (Table S2). For the 48 deployments using the active compensator, reliability was lower, with 15 deployments (~31 %) behaving as expected, i.e. recovering at pressures above 90 % of *in situ* values. Within the remaining deployments, 27 (~56 %) still remained above 75 % retention of *in situ* pressure, and only 3 (~ 6 %) failed to retain more than 50 % of *in situ* pressure values.

The following results focus on the pressure history inside the PERISCOP PRD during its operation, from the moment it leaves the bottom, ascends through the water column, further reaches the surface, is hauled on board ship, and finally opened after releasing the pressure. For clarity, only 50 deployments are presented here, and while all the deployments using passive compensation are presented, only some of the successful deployments are shown regarding the use of active compensation. The data shown correspond either to technical deployments in Mediterranean waters in winter, i.e. with a temperature gradient of less than 2°C between bottom and surface waters (almost isothermal water column, Table S1), or to scientific deployments at MAR vent sites, with a temperature gradient of about 20 °C between bottom and surface waters (non-isothermal water column, Table S2).

Operating in an isothermal water column (Mediterranean Sea, Figure 7-8, Table S1)

All 12 deployments in this area were technical tests, in order to train the submersible crews to manipulating the PERISCOP PRD *in situ*, and to evaluate the pressure-retaining performance of different compensators, in the absence of significant heat transfer, due to an almost isothermal water column (less than 2°C gradient between sampling site and surface water, see temperature data in Figures 7-8). The autonomous pressure/temperature probe fixed on the shuttle (see Figure 4E) provides the pressure prevailing around the PRD, and the temperature of the surrounding water column, and therefore allows tracking of the different steps during recovery (Figure 7). Figure 7 shows pressure and temperature data throughout a deployment using the active compensator (Deployment # P6, EssNaut 2016 cruise, see Table S1). Throughout the process, the pressure inside the PRD remained above 97.6 % of in *situ* pressure (bold blue line), and reached 98.3 % just before pressure was released on ship deck (indicated by arrow 3). Interestingly, when the shuttle was launched, meaning that the PRD began its ascent towards the surface (indicated by arrow 1), the pressure prevailing inside the PRD followed that of the surrounding water column, until about 1 MPa was lost. After this loss, corresponding to an ascent of about 100 m through the water column, the pressure in the PRD stabilized.

Figure 8 shows pressure and temperature data throughout a deployment with no pressure compensation (Deployment # P5, EssNaut 2021 cruise, see Table S1). Throughout the process, the pressure inside the PRD remained above 65.2 % of in *situ* pressure (bold blue line), and reached 66.6 % just before pressure was released on ship deck (indicated by arrow 3). As for all the recoveries presented in this work, when the PRD began its ascent towards the surface (indicated by arrow 1), the pressure inside the PRD first followed that of the surrounding water column, until about 1 MPa was lost. After this loss corresponding to an ascent of about 100 m through the water column, the pressure continued to decrease, but following a lower rate. When the shuttle (and PRD) reached the surface (indicated by arrow 2), the pressure inside the PRD reached its minimum value, before slightly increasing until pressure release (indicated by arrow 3), 36 minutes after the shuttle had reached the surface.

Generally, for the 7 deployments using the active compensator (Table S1), minimum pressure retention ranged from 93.8 to 97.6 %, upon reaching surface waters, and final pressures upon release ranged from 93.9 to 98.3 %. When the passive compensator was used, and loaded with oil (3 deployments, Table S1), minimum pressure retention ranged from 83.3 to 84.4 %, upon reaching surface waters, and final pressures upon release ranged from 86.7 to 89.1 %. When no compensation was used (two deployments, see Table S1), the minimum pressure retention was 63.5 and 65.2 % of *in situ* values, and final pressures upon release 60.1 and 66.6 % respectively.

Sampling in a non-isothermal water column (MAR sites, Table S2, Figures 9 to 12)

Most of the deployments presented here involved sampling of fauna, mainly hydrothermal vent shrimps (see Figure 5A, Figure 6 A, B). Which ever compensation system was employed (including absence of compensation), all deployments resulted in samples in apparently very good physiological condition, as suggested by the highly active behavioural response just after decompression of the PRD. This opposes to the weak activity of shrimps collected without pressure retention, with only slow and uncoordinated movements for shrimps originating from the Rainbow site at about 2300 m depth, and almost total absence of motion, suggesting moribund or dead organisms, in the case of deeper sites beyond 3000 m depth (TAG, Snake Pit, Broken Spur, see Table S2).

The thermal conditions encountered during these MAR cruises corresponded to cold bottom waters, and warmer surface waters: 3.5 / 24 °C for the Rainbow site (2300 m depth), for bottom and surface water temperatures respectively, 2.6 / 23 °C for the TAG site (3600 m depth), 2.5 / 23 °C for the Snake Pit site (3400 m depth), and 3 / 26 °C for the Broken Spur site (3100 m depth). Temperature gradients between bottom and surface waters therefore ranged from + 20.4 to + 23 °C.

Figure 9 shows pressure and temperature data throughout a deployment using the active compensator (Deployment # D5, MomarDream cruise, see Table S2). Throughout the process, the pressure inside the PRD remained above 97.6 % of *in situ* pressure (bold blue line), and reached 103.5 % just before pressure was released on ship deck (indicated by arrow 3). As for all recoveries presented in this work, when the PRD began its ascent towards the surface (indicated by arrow 1), the pressure prevailing inside the PRD first followed that of the surrounding water column, until about 1 MPa was lost. After this loss corresponding to an ascent of about 100 m through the water column, the pressure in the PRD stabilized. When the shuttle (and PRD) reached the surface (indicated by arrow 2), the pressure inside the PRD increased by approximately 1 MPa in a few minutes, before it stabilised again. It can be seen here that the water column was gradually warmer as depth decreased (thin red line). For this deployment, an additional autonomous temperature probe was inserted inside the sampling cell (where collected organisms are stored), and allowed to observe gradual warming of the sample, reaching about 17 °C upon final pressure release (indicated by arrow 3), almost 50 minutes after the shuttle had reached the surface.

Figure 10 shows pressure and temperature data throughout a deployment using the passive compensator, filled with water (Deployment # P6, Bicose 2 cruise, see Table S2). Throughout the process, the pressure inside the PRD remained above 84.5 % of *in situ* pressure (bold blue line), and reached 94 % just before pressure was released on ship deck (indicated by arrow 3). As for all recoveries presented in this work, the ~1 MPa pressure loss is observed at the beginning of the shuttle ascent, followed by pressure decrease at lower rate. When the shuttle (and PRD) reached the surface (indicated by arrow 2), the pressure inside the PRD reached its minimum value, before gradually increasing until pressure release (indicated by arrow 3), 38 minutes after the shuttle had reached the surface.

Figure 11 shows pressure and temperature data throughout a deployment with no pressure compensation (Deployment # P16, Bicose 1 cruise, see Table S2). Throughout the process, the pressure inside the PRD remained above 72.4 % of in *situ* pressure (bold blue line), and reached 79.3 % just before pressure was released on ship deck (indicated by arrow 3). As for all recoveries presented in this work, the ~1 MPa pressure loss is observed at the beginning of the shuttle ascent, followed by pressure decrease at lower rate. When the shuttle (and PRD) reached the surface (indicated by arrow 2), the pressure inside the PRD reached its minimum value, before gradually increasing until final pressure release (indicated by arrow 3), 16 minutes after the shuttle had reached the surface.

Finally, Figure 12 displays the final pressure values inside the PRD just before pressure was released on the deck of the ship (i.e. for access to samples, see Table S2), as a function of time since the shuttle had reached the warm surface waters (also in Table S2). These values are compared to the mean of minimum pressures (red points), which occurred either when the shuttle reached the surface (passive or no compensation) or before (active compensation), and are therefore positioned on the vertical axis of the graph (Time is 0 minutes when reaching the surface). These minimum values (mean % +/- SD) are 72.3 +/- 0.5 (n = 5) for no compensation, 84.2 +/-1.3 (n = 22) for water-filled passive compensation, 91.0 +/- 0.3 for oil-filled compensation (n = 3), and 97.9 +/-0.3 for active compensation (n = 4).

For all types of compensation, pressure generally increased after the PRD had reached the surface. The lowest variations were observed for active compensation (triangles), while the highest were those occurring in the case of oil-filled compensation, which may have exceeded 116 % of *in situ* pressure (squares). In the case of water-filled compensation or in the absence of compensation (plain and empty circles respectively), final pressure always remained below 100 % of *in situ* pressure, even after almost one hour of delay after reaching the surface.

DISCUSSION

Overview

Although most of the following discussion focuses on pressure compensation issues, other aspects of PERISCOP deployments should first be addressed: the sea-going experience presented here confirms the efficiency of the general principle, i.e. the use of a submersible-assisted sampling (either R.O.V. or H.O.V., Shillito et al, 2008). This has allowed scientists to target species, as initially experienced by pioneering work of Koyama et al (2002), a clear advantage compared to using baited traps, the latter method being uncertain regarding effective capture, and strictly restricted to mobile fauna. Our choice to achieve collection by using sub-sampling cells (Periscopette or Croco sampling cells) prior to recovery (in the PRD) proved its efficiency. The small size and weight of these cells clearly increases manoeuvrability during the sampling action *in situ*. Moreover, because the submersible does not have to transport the whole PRD (unlike the PRD described in Koyama et al, 2002), it leaves more possibilities for other experiments to be carried out during dives, which in turns facilitates the regular use of isobaric sampling deployments, within the tight time schedule of an oceanographic cruise. Last, this method probably increased the reliability of an effective sealing of the PRD's globe-valve (see Figures 5 and 6), since the introduction of a calibrated sub-sampling cell into the PRD helped to prevent the samples or associated particles from getting stuck across the closing seals. Deficient sealing of a PRD's main aperture, in relation to sample introduction, is indeed a most likely cause of leakage (see discussion in Jackson et al, 2017, and Case et al, 2017).

Finally, as initially introduced by Bianchi et al (1999), the systematic use of pressure data recording (both inside and outside of the PRD) throughout the entire sampling cycle is to be encouraged (as in Garel et al, 2019, Wang et al, 2022), because it proved very helpful in detecting misfunction, and also because it revealed that the final pressure (i.e. when the PRD was back on board the ship) was not necessarily the lowest experienced during the process.

Analysis of pressure history inside the PRD during recovery, without pressure compensation

When attempting to retrieve samples from deep waters inside a sealed container, pressure variations are likely to occur, and depend on several phenomena, which have long been documented (MacDonald, 1975, Yayanos, 1978). During the ascent of the pressure-retaining device (PRD) towards the surface, the pressure prevailing in the surrounding environment decreases. Provided there is no leakage due to seal failure, the hydrostatic pressure inside the PRD drops because of the initial movement and compression of elastomer seals which ensure sealing of the PRD, and because of the following elastic expansion of the metallic PRD walls (see ANNEX 1 for more detail). Both phenomena cause an increase of the internal volume of the PRD, and consequently an expansion of the seawater trapped inside the PRD, resulting in significant pressure drops. On the contrary, a temperature rise expected when reaching warm surface waters may result in increased pressure inside the PRD. Although this may compensate for pressure losses described above, this phenomenon should be avoided as much as possible, on physiological grounds (MacDonald, 1975, Childress et al, 1978)

The pressure loss due to seals depends mainly on the volume variation due to the positioning of seals within their respective grooves, and at lesser extent on deformation of seals while being compressed, once the final sealing position is reached. In our study, we estimated that the movement of seals would result in a pressure loss of ~1 to 1.5 MPa at 5°C, whatever working pressure was envisaged. The pressure loss due to the expansion of the PRD metallic walls was experimentally estimated at the laboratory, in isothermal conditions, and predicted to be about 26% of working pressure, at 4°C (see ANNEX 1). From there, accounting for seal movement, it would appear that the PERISCOP would theoretically retain about 70 % of *in situ* pressure when operated at 36 MPa (3600 m depth), and about 63 % when operated at 12 MPa (1200 m depth), in isothermal conditions.

Figures 8 and 11 allow to observe the pressure-retaining performance of the PRD alone, when no pressure compensation system is employed. The data are in relatively good agreement with predictions, minimum pressure values reaching respectively 65.2 and 72.4 % retention of *in situ* pressure, measured for deployments at 1250 and 3620 m depths respectively. In the first seconds of the PRD ascent, pressure drops at the same rate as the surroundings, as if the PRD was still in an open position. In fact, this behaviour likely corresponds to the seals moving across the grooves inside which they are housed, at almost equal pressures on both sides of seals, until they are blocked against the groove edge. It is only then that they reach an effective sealing position, allowing a difference of pressures to build up. Later during the ascent, the PRD walls gradually expand proportionally to the decrease of surrounding pressure, which stabilizes when the PRD reaches the surface. From then on, the pressure inside the PRD may change because of thermal conditions. In the case of an almost isothermal water column (Figure 8, about + 2°C gradient) the pressure increase is small (~ + 1.5 % after almost 40 min in surface waters), while it is more important (~ + 7 % after only 16 min in surface waters) when surface waters are warm (Figure 11, about + 20°C gradient).

Analysis of pressure history inside the PRD during recovery, using pressure compensation

Comparison of deployments with or without pressure compensation can be done for similar thermal conditions (non-isothermal water column, red points in Figure 12, and Table S2). The best pressure-retaining performance is obtained when using the active compensator (about 98 % of *in situ* pressure, Figure 12). The use of passive compensation (oil- or water-filled modes) leads to a lower minimum pressure-retaining performance (91 % and 84 % respectively). Both methods (passive and active) however improve the pressure-retaining performance of the PERISCOP PRD, which retains a minimum pressure of about 72 % of in *situ* pressure, when no compensation is used. Additionally, the active system seems less sensitive to the impact of warming on pressure, since it displays the smallest pressure increase after reaching warm surface waters. The reference container inside the active compensator is probably less subject to thermal variation and subsequent pressure increase, and therefore drives the release of seawater from the PRD as gradual heating of the latter occurs. On the contrary, the passive compensator is more sensitive to thermal conditions encountered in warm surface waters, particularly when using oil-filled compensation, as discussed below.

Reliability is an important issue when considering repeated use of pressure-retaining sampling. The initial compensation system (active) presented by Shillito et al (2008) gradually gained in reliability, through improvements described above. Indeed, the integration of the differential valves inside the compensator's main container was a progress: their functioning (opening and/or closing) became more reproducible, probably because they were then submitted to a constant external pressure (atmospheric), and also to more stable thermal conditions, throughout the sampling process. However, such a compensator still involves more complex connections (compare figures 2 and 3), and requires more operations than the passive system (both *in situ* and on board the ship). The active system therefore requires more attention (maintenance) in order to reproduce regular functioning. On the contrary, the passive system may be less efficient in terms of pressure retention, but its more simple design increases reliability and ease of operation.

The use of oil for passive pressure compensation

We made a few deployments using an oil-filled passive compensator, which performs better than its water-filled analog in similar conditions (non-isothermal water column), regarding the minimum pressure (see red points in Figure 12). This improvement is due to the higher compressibility coefficient of silicon oil, with respect to water (Kiyama et al, 1953, Fine and Millero, 1973). However, this oil-filled mode seems more sensitive to heating and subsequent pressure rise upon reaching warm surface waters (Figure 12). The pressure increase due to overheating of a trapped liquid is dependant on the ratio between the thermal expansion coefficient of a given liquid, and its isothermal compressibility coefficient (Ramirez et al, 2010). The thermal expansion coefficient of commercially-available silicon oils is typically 5 to 15-fold that of water, while their compressibility coefficients are about two to four-fold that of water (Kiyama et al, 1953, Fine and Millero, 1973, see also Ramirez et al, 2010). Consequently, the ratio between the thermal expansion and the isothermal compressibility coefficients is likely to be more important for silicon oil than for water, thus leading to increased overpressure upon warming in surface waters. Therefore, although the use of oil as a compensating fluid is promising in terms of pressure compensation, the thermal insulation of the passive compensator should be improved in the future, in order to limit the potential for overpressure. Ultimately, provided efficient thermal insulation is achieved, this tendancy for overpressure could be used in the future as a means of compensating pressure losses in the

PRD through controlled heating of an oil-filled passive compensator. Our group is currently exploring this possibility.

Comparison with other PRDs and their conventional (gas-loaded) compensation systems

Most other PRDs used in the field of geology, microbiology, or studies of larger fauna, involve the use of gaseous-nitrogen-loaded pressure accumulators, in order to compensate for pressure losses during recovery. Such systems are efficient, and help maintain pressures close to *in situ* values. The general principle is explained in MacDonald (1975) and Yayanos (1978). Schematically, the volume increase due to seal movement and container expansion leads to a loss in pressure, which is inversely proportional to the enclosed volume V, and to the isothermal compressibility coefficient B of the enclosed fluid ($(\delta P / \delta V)_T = - 1 / (B \times V)$). The principle is therefore to increase the volume and compressibility of the enclosed medium, by adding a highly compressible gaseous component to the system. Ideally, the gas quantity should be maximised at operating pressure (the pressure encountered at sampling depth), implying an initial loading pressure slightly inferior to the operation pressure (i.e. about 90 %). Using a gas accumulator, Garel et al (2019) maintained +/- 5% of *in situ* pressures in microbial samplings from 3000 m depth, as evidenced by constant recording of pressure history throughout the sampling process. Workers in the same group had earlier shown that their compensation system could improve by about 25% the performance of their samplers (Bianchi et al, 1999). Using a much larger fish sampler (90 l), Drazen et al (2005) retained about 93-95 % of *in situ* pressure, following recoveries from 1350-1500 m depths. Many other examples have been recently reviewed by MacDonald (2021). Overall, in terms of pressure-retaining performance, while the active compensator presented in this work (94% pressure retention at the lowest) compares well with nitrogen accumulators mentioned above, the passive compensator seems somewhat less efficient (around 80% at the lowest, for water-filled compensator). However, unlike the passive compensator, the gaseous accumulators and our active compensator both need to be pressurised prior to deployment. Moreover, in the case of gas-loaded accumulators, such a pressurisation may prove unpractical to achieve when targeting loading pressures above 20-30 MPa, i.e. pressures above those readily available in commercially-used nitrogen cylinders. Additionally, it should be recalled that because of their elevated internal energy (compared to pressurised liquids), pressurised gases may present more safety issues for users.

The passive compensator, in its water-filled version, involves the elasticity of its internal container (Figure 3), and acts as a loaded mechanical "spring" which sends seawater back to the PRD as the latter expands. When compressible silicon oil is used, a function similar to that of a gas accumulator is added, through the introduction of a fluid more compressible than water. While silicon oil remains significantly less compressible than nitrogen gas, even at high pressures (about 10 to 3 fold lower, between 10 and 110 MPa, Ramirez et al 2010, Kiyama et al 1953, Priede, 2018), it nevertheless remains a significant contribution to the decrease of the $(\delta P / \delta V)_T$ term mentioned above. In addition, the large volume involved (4 L for the compensator internal container, while the PRD has a volume of 6 L, resulting in a total 10 L volume) also participates to reducing this term.

Pressurised recovery at hadal depth

The PERISCOP PRD and its compensator systems were not designed for hadal depths of operation (beyond 6000 m), the deepest recoveries occurred from 3650 m depths on the Mid-Atlantic Ridge. Designing a new PRD based on the PERISCOP, but upgraded at higher working pressures, is a current challenge, because large volumes (PERISCOP has a 10 cm diameter opening, for more than 6 L volume) and realistic PRD wall thicknesses (in order to respect maximum weight constraints) will necessarily require that pressure losses are compensated for. It is likely that an active system may prove difficult to design, especially if loading pressures above 110 MPa are required (in the high-pressure reservoir, see methods section). Alternatively, we believe that the general principle of a passive liquid-filled compensator may prove quite efficient for hadal use. Recently, Wang et al (2022) maintained about 80-85% of *in situ* pressure during sampling of amphipods in a relatively small PRD (about 0.7 L volume), at the bottom of the Mariana trench (10900 m depth). They used a hybrid compensation system, by firstly using a liquid injector to push the seals towards their sealing position, and secondly using a nitrogen accumulator pre-loaded at 30 MPa, a pressure which can be reasonably reached by using commercially available pressurised nitrogen bottles. Increasing the loading gas pressure would probably improve the performance of their system, but would prove unpractical, if not hazardous. Moreover, the pressure-retaining performance obtained by these authors, although lower than theoretically expected, could prove sufficient to insure good physiological conditions of the samples (although their trials resulted in 100% mortality of samples, this was likely due to overheating in surface waters, rather than insufficient pressure compensation (see Yayanos, 1978, 2009)). A liquid-filled passive compensator such as presented here would not require pre-loading. Of course, the design of such an instrument would require that sufficient volume and elasticity of its internal container is involved, and that buckling issues are accounted for, regarding its external container. We advocate that future samplers will tend to increase in volume, in order to envisage broader sampling capacities, and propose that passive liquid compensators will prove more appropriate for such uses. As discussed above, and in the following lines, thermal insulation remains a major issue in deep-sea sampling of live fauna, but also for the stability of a liquid-filled compensator, should liquids such as silicon oil be employed (Figure 12).

Is full pressure compensation necessary ? What about thermal insulation ?

The PERISCOP PRD has mostly been used at depths greater than 1000 m, and while some of the deployments occurred in Mediterranean waters (technical deployments), most faunal samplings were achieved at hydrothermal vent sites (Mid-Atlantic Ridge, and East Pacific Rise), mainly at depths between 1700 and 3600 m. Several thousand organisms were thus recovered, representing various taxa. Before its reliability was improved, it is the active compensator that was responsible for most misfunctions. However, even when pressure-retaining performance was as low as 65 % (either no compensation or compensation partial misfunction), most organisms were recovered in apparent very good physiological conditions, as suggested by their generally active behaviour responses (see biological studies mentioned in results). This was not always the case for fauna recovered without pressure: while most vent organisms recovered from 1700 m depths (Lucky Strike vent field) possibly survived several weeks, if not months, at atmospheric pressure (Shillito et al, 2015, 2020), deeper-originating fauna were more impacted. *Rimicaris exoculata* vent shrimps from depths around 2300 m (Rainbow vent field) still appeared fairly active upon recovery, but sometimes displayed uncoordinated movements, and although they were generally responsive to mechanical stimulation, their activity would gradually fade in a matter of one to two days. On the contrary, shrimps of the same species, but originating from deeper sites (beyond 3000 m depth), were usually recovered in a motionless state, appearing moribund, with weak and uncoordinated responses to stimulation. For these organisms, re-pressurisation in dedicated laboratory pressure aquaria often failed to restore normal behaviour. Low tolerance to full decompression has been reported for other species (Treude et al, 2002, Ravaux et al, 2013), and Pradillon (2012) had already mentioned that 2000 m depth could be a physiological obstacle for survival to decompression. Other authors have also discussed this point (Brown and Thatje, 2014).

Still, many studies involving isobaric sampling (including ours) report on the fact that full pressure recovery is not always reached, and that recovery at partial pressure is tolerated by many taxa (including fish, Koyama et al, 2002), even among the deepest occurring ones (Peoples et al, 2019, Yayanos, 1981, 2009). Additionally, highly performant compensation systems such as the active compensator we present are an example of the increasing complexity (in both design and operation) required to obtain full pressure recovery, compared to the passive compensator. The latter is of much more practical use, significantly lower cost, and its simplicity implies increased reliability on the long term, in addition to the absence of pressurised gas, which significantly increases the safety of pressure-manipulating procedures. Such simple cheap and safe equipments could then become widespread among the community of deep-sea scientists, including for use in hadal environments.

In future developments of PRDs, recovery in isothermal conditions should not be overlooked. The vent fauna reported in this work are mostly quite eurythermal (see Bates et al, 2010, Van Dover, 2019), and therefore tolerate temperature increases which occur when the PRD reaches surface waters (Figure 9). Such tolerance is unlikely to occur with stenothermal fauna originating from colder environments, since thermal challenge has long been identified as a major cause of trauma during deep-sea sampling (Childress et al, 1978, Wilson and Smith, 1985, Wang et al, 2022). This underlines the necessity of improving thermal insulation for our equipment. We are in test phase for additional thermal insulation of the main globe-valve of our PRD, which is a major thermal bridge with the surrounding environment.

CONCLUSIONS

We here presented an update of the PERISCOP pressure retaining device (PRD), which was improved since its initial design, and which operation is now close to routine. The data and practical experience we acquired at sea, lead us to propose the following conclusions, which we hope may help other investigators in the design and operation of future PRDs.

1) Pressure and temperature history inside the PRD throughout the sampling cycle should be recorded.

2) Active sampling with a submersible (as opposed to trapping based on attraction to bait) allows to target species, and therefore significantly widens scientific perspectives.

3) Full pressure retention throughout PRD operation is not always reached, however pressure retention as low as 65% may suffice for recovering live samples. This would allow for further physiology experiments in dedicated aquaria to take place, after restoring full *in situ* pressure.

4) The use of gas-free pressure compensators should be encouraged, because increased safety leads to more practical and wide use by biologists, and because gas-loaded systems may prove of limited efficiency as sampling depth increases beyond 3000 m depths.

5) Passive compensators such as presented here are safe and easy to use, and relatively cheap. Moreover, we advocate that they may be effective tools at hadal depths. The more complex (but more efficient) active compensator may still be envisaged in particular cases of pronounced intolerance to decompression.

6) Finally, thermal insulation should not be overlooked, in many cases surface waters are much warmer than deep environments, and this may lead to serious trauma, even on pressure-recovered samples.

Pioneering works on the effects of pressure on living organisms started way back in the 19th and 20th centuries (Draper and Edwards, 1932, Sébert, 2002 for review), but physiological studies on live deep-sea animals in laboratory conditions are still in their infancy. One reason for this is that sampling in the deep-sea and further maintaining *in situ* pressure conditions at the laboratory, are challenging issues, on both technical and financial grounds. However, because the biology of deep fauna remains largely unknown, and because the field of investigations is therefore so wide, we believe that undertaking such studies is a very rewarding process, and an urgent matter in the face of growing human impacts on the Deep Biosphere. A main objective of the work presented herein, is to incite a wide community of marine biologists to realize that such studies are feasible, and necessary.

ACKNOWLEDGEMENTS

We wish to warmly thank the captains and crews of the Ifremer oceanographic ships N/O Atalante and N/O Pourquoi Pas?, along with the crews of the manned submersible “Nautile”, and the ROV “Victor 6000”, for their dedication in achieving deep-sea sampling. We are also grateful to M. Zbinden and J. Ravaux for their scientific contributions, and to chief scientists of the cruises where PERISCOP was deployed (Momareto 2006, MomarDream 2007, Mescale 2010, Mescale 2012, Biobaz 2013, Bicose-1 2014, EssNaut 2016, Bicose-2 2018, Transect 2018, EssNaut 2021). We thank the reviewers for their help in improving this manuscript. The PERISCOP project was initially funded by the European Community program EXOCET/D (6^{th} Framework Programme - Grant Agreement 505342, 2004-2006). Upgrades benefited from the programs BALIST ANR-08-BLAN-0252 (2008-2011), BQR UPMC (2008), the European Community Program MIDAS (7th Framework Programme - Grant Agreement 603418, 2014-2016), and the CNRS program “Instrumentation aux limites” (2016).

REFERENCES

Auguste, M., Mestre, N. C., Rocha, T. L., Cardoso, C., Cueff-Gauchard, V., Le Bloa, S., Cambon-Bonavita, M. A., Shillito, B., Zbinden, M., Ravaux, J., Bebianno, M. J. (**2016**) Development of an ecotoxicological protocol for the deep-sea fauna using the hydrothermal vent shrimp *Rimicaris exoculata*. *Aquatic Toxicology*, **175**, 277-285

Bates A.E., Lee R.W., Tunnicliffe V., Lamare M.D. (2010) Deep-sea hydrothermal vent animals seek cool fluids in a highly variable thermal environment. *Nature Communications*, **1**:14‑16. https://doi.org/10.1038/

Bianchi, A., Garcin, J., Tholosan, O. (**1999**) A high-pressure sampler to measure microbial activity in the deep sea. *Deep-Sea Research I,* **46**, 2129–2142.

Brown, A., Thatje, S. (**2014**) Explaining bathymetric diversity patterns in marine benthic invertebrates and demersal fishes: physiological contributions to adaptation of life at depth. *Biological Reviews*, **89**, 406–426. https://doi.org/10.1111/brv.12061.

Case, D.H., Ijiri, A., Morono, Y., Tavormina, P., Orphan, V.J., and Inagaki, F. (**2017**) Aerobic and Anaerobic Methanotrophic Communities Associated with Methane Hydrates Exposed on the Seafloor: A High-Pressure Sampling and Stable Isotope-Incubation Experiment. *Frontiers in Microbiology,* **8**:2569. doi: 10.3389/fmicb.2017.02569

Childress, J.J., Barnes, A.T., Quetin, L.B., Robison, B.H. (**1978**) Thermally protecting cod ends for the recovery of living deep-sea animals *Deep-Sea Research*, Vol. **25**, 419-422.

Draper, J.W. and D.J. Edwards (**1932**) Some effects of high pressure on developing marine forms. *Biological Bulletin of marine biology Labortory, Woods Hole* **63**, 99-107

Drazen, J.C., Bird, L.E., Barry, J.P. (**2005**) Development of a hyperbaric traprespirometer for the capture and maintenance of live deep-sea organisms. *Limnology and Oceanography: Methods* **3**, 488 - 498.

Duperron, S., Quiles, A., Szafranski, K. M., Léger, N., Shillito, B. (**2016**) Estimating symbionts abundances and gill surface areas in specimens of the hydrothermal vent mussel *Bathymodiolus puteoserpentis* maintained in pressure vessels. *Frontiers in Marine Science*, **3** : 16, doi: 10.3389/fmars.2016.00016

Fang, J., Zhang, L., and Bazylinski, D.A. (**2010**) Deep-sea piezosphere and piezophiles: geomicrobiology and biogeochemistry. *Trends in Microbiology* **18**, 413-422.

Fine R. A., Millero, F. J. (**1973**) Compressibility of water as a function of temperature and pressure. *Journal of Chemical Physics*, **59**, 10, 5529-5536

Garel, M., Bonin, P., Martini, S., Guasco, S., Roumagnac, M., Bhairy, N., Armougom, F. and Tamburini, C. (**2019**) Pressure-Retaining Sampler and High-Pressure Systems to Study Deep-Sea Microbes Under in situ Conditions. *Frontiers in Microbiology,* **10**:453. doi: 10.3389/fmicb.2019.00453

Jackson, K., Witte, U., Chalmers, S., Anders, E., Parkes, J. (**2017**) A System for Retrieval and Incubation of Benthic Sediment Cores at In Situ Ambient Pressure and under Controlled or Manipulated Environmental Conditions. *Journal of Atmospheric and Oceanic Technology*, **34** (5), 983-1000
doi : 10.1175/JTECH-D-16-0248.1

Kiyama, R., Teranishi, H., Inoue, K. (**1953**) The compressibility measurements on liquids. *The Review of Physical Chemistry of Japan*, 23(1): 20-29

Koyama, S., Miwa, T., Horii, M., Ishikawa, Y., Horikoshi, K., Aizawa, M. (**2002**) Pressure-stat aquarium system designed for capturing and maintaining deep-sea organisms. *Deep-Sea Research I,* 49, 2095–2102.

Le Bloa, S., Boidin-Wichlacz, C., Cueff-Gauchard, V., Rosa, R.D., Cuvillier-Hot, V., Durand, L., Methou, P., Pradillon, F., Cambon-Bonavita, M.-A. and Tasiemski, A. (**2020**) Antimicrobial Peptides and Ectosymbiotic Relationships: Involvement of a Novel Type IIa Crustin in the Life Cycle of a Deep-Sea Vent Shrimp. *Frontiers in Immunology* 11:1511.
doi: 10.3389/fimmu.2020.01511

MacDonald, A.G. (**1975**) "Deep sea Bio-engineering", in Physiological aspects of deep sea biology, Monographs of the Physiological Society 31, pp. 1-434, Cambridge University Press

MacDonald, A.G. (**2021**) "The Effects of Decompression and Subsequent Re-compression on the Activity of Deep-Sea Animals and Eukaryote Cells. The Isobaric Collection of Deep-Sea Animals". In Life at High Pressure. In the Deep Sea and Other Environments. Springer Nature Switzerland
doi: 10.1007/978-3-030-67587-5

Methou, P., Hernández-Ávila, I., Aube, J., Cueff-Gauchard, V., Gayet, N., Amand, L., Shillito, B., Pradillon, F., and Cambon-Bonavita, M.-A. (**2019**) Is It First the Egg or the Shrimp? – Diversity and Variation in Microbial Communities Colonizing Broods of the Vent Shrimp *Rimicaris exoculata* During Embryonic Development. *Frontiers in Microbiology,* **10**:808.
doi: 10.3389/fmicb.2019.00808

Papot, C., Massol, F., Jollivet, D., Tasiemski, A. (**2017**) Antagonistic evolution of an antibiotic and its molecular chaperone: how to maintain a vital ectosymbiosis in a highly fluctuating habitat. *Scientific Reports*, **7** : 1454, doi :10.1038/s41598-017-01626-2

Peoples, L.M., Norenberg, M., Price, D., McGoldrick, M., Novotny, M., Bochdansky, A., Bartlett, D.H. (**2019**) A full ocean depth rated modular lander and pressure retaining sampler capable of collecting hadal-endemic microbes under in situ conditions. *Deep-Sea Research, Part I*, **143**, 50–57.
doi : 10.1016/j.dsr.2018.11.010

Piquet, B., Shillito, B., Lallier, F.H., Duperron, S., Andersen, A.C. (**2019**) High rates of apoptosis visualized in the symbiont-bearing gills of deep-sea *Bathymodiolus* mussels. *PLoS ONE* **14**(2): e0211499.
doi : 10.1371/journal.pone.0211499

Piquet, B., Lallier, F.H., André, C. Shillito, B., Andersen, A.C., Duperron, S. (**2020**) Regionalized cell proliferation in the symbiont-bearing gill of the hydrothermal vent mussel *Bathymodiolus azoricus*. *Symbiosis*.
doi : 10.1007/s13199-020-00720-w

Pradillon, F. (**2012**) High hydrostatic pressure environments. In: Bell, E.M. (Ed.), Life at Extremes: Environments, Organisms and Strategies for Survival. CABI, Wallingford, pp. 271–295. https://doi.org/10.1079/9781845938147.0271.

Priede, I.G. (**2018**) Buoyancy of gas-filled bladders at great depth. *Deep-Sea Research Part I*, **132**, 1-5. doi.org/10.1016/j.dsr.2018.01.004

Ramirez, J.C., Ogle, R.A., Carpenter, A.R., Morrison, D. (**2010**) Preventing Overpressure Hazards from Trapped Liquids. *Process Safety Progress*, **29**, No.4, 313-317
doi : 10.1002/prs.10413

Ramirez-Llodra, E., Brandt, A., Danovaro, R., De Mol, B., Escobar, E., German, C.R., Levin, L.A., Martinez Arbizu, P., Menot, L., Buhl-Mortensen, P., Narayanaswamy, B.E., Smith, C.R., Tittensor, D.P., Tyler, P.A., Vanreusel, A., and Vecchione, M. (**2010**) Deep, diverse and definitely different: unique attributes of the world's largest ecosystem. *Biogeosciences*, **7**, 2851–2899, doi:10.5194/bg-7-2851-2010

Ramirez-Llodra, E., Tyler ,P.A., Baker, M.C., Bergstad, O.A., Clark, M.R., et al. (**2011**) Man and the last great wilderness: human impact on the deep sea. *PLoS One 6 (7),* e22588. http://dx.doi.org/10.1317/journal.pone.0022588.

Ravaux, J., Machon, J., Shillito, B., Barthélémy, D., Amand, L., Cabral, M., Delcour, E., Zbinden, M. (**2021**) Do Hydrothermal Shrimp Smell Vents ? *Insects,* **12**, 1043.
doi : 10.3390/insects12111043

Ravaux, J., Léger, N., Hamel, G., Shillito, B. (**2019**) Assessing a species thermal tolerance through a multiparamer approach: the case study of the deep-sea hydrothermal vent shrimp *Rimicaris exoculata*. *Cell Stress and Chaperones*, **24** : 647–659.
doi : 10.1007/s12192-019-01003-0

Ravaux, J., Hamel, G., Zbinden, M., Tasiemski, A.A., Boutet, I., Léger, N., Tanguy, A., Jollivet, D., Shillito, B. (**2013**) Thermal limit for metazoan life in question: *in vivo* heat tolerance of the Pompeii worm. *Plos One*, 8(5): e64074. doi: 10.137/journal.pone.0064074

Ravaux, J., Cottin, D., Chertemps, T., Hamel, G., Shillito, B. (**2009**) "Hydrothermal vent shrimps display low expression of the heat-inducible hsp70 gene in nature", *Marine Ecology Progress Series*, **396**, 153-156.

Sébert, P. (**2002**) Fish at high pressure: a hundred year history. *Comparative Biochemistry and Physiology* 131A, 575–585.

Shillito, B., Hamel, G., Duchi, C., Cottin, D., Sarrazin, J., Sarradin, P.M., Ravaux, J., Gaill, F. (**2008**) "Live Capture of Megafauna from 2300 m Depth, Using a Newly-Designed Pressurised Recovery Device", *Deep-Sea Research Part I*, **55**, 881-889.

Shillito, B., Gaill, F., Ravaux, J. (**2014**) “The IPOCAMP pressure incubator for deep-sea fauna”, *Journal of Marine Science and Technology (Taiwan)*, Vol. **22**, No. 1, pp. 97-102. doi: 10.6119/JMST-013-0718-3

Shillito B., Ravaux J., Sarrazin J., Zbinden M., Sarradin P.M., Barthelemy D. (**2015**) Long-term maintenance and public exhibition of deep-sea hydrothermal fauna : the AbyssBox project. *Deep-Sea Research, Part II*, **121**, 137-145. doi : 10.1016/j.dsr2.2015.05.002.

Shillito, B., Desurmont, C., Barthélémy, D., Farabos, D., Després, G., Ravaux, J., Zbinden, M., Lamazière, A. (**2020**) Lipidome variations of hydrothermal vent shrimps according to acclimation pressure : a homeoviscous response ? *Deep-Sea Research Part I*, 161. doi : 10.1016/j.dsr.2020.103285

Sweetman, A.K., Thurber, A.R., Smith, C.R., Levin, L., Mora, C., Wei, C., Gooday, A.J., Jones, D., Rex, M., Yasuhara, M. et al (**2017**) Major impacts of climate change on deep-sea benthic ecosystems. *Elementa Science of the Anthropocene*, 5: 4, doi: https://doi.org/10.1525/elementa.203

Szafranski, K.M., Piquet, B., Shillito, B., Lallier, F.H., Duperron, S. (**2015**) Relative abundances of methane- and sulfur-oxidizing symbionts in gills of the deep-sea hydrothermal vent mussel *Bathymodiolus azoricus*: effect of isobaric recovery. *Deep-Sea Research, Part I*, **101**, 7-13.

Treude, T., Janβen, F., Queisser, W., Witte, U. (**2002**) Metabolism and decompression tolerance of scavenging lysianassoid deep-sea amphipods. *Deep-Sea Research Part I,* **49**, 1281–1289

Van Dover, C. L. (**2019**) Forty years of fathoming life in the ocean depths. *Nature*, **567**, 182-183

Wang, H., Chen, J., Cao, C., Ge, Y., Fang, J., Zhou, P., Lin, P. (**2022**) Capturing amphipods in the Mariana Trench with a novel pressure retaining sampler. *Deep-Sea Research Part I* 184 103772 doi: 10.1016/j.dsr.2022.103772

Wilson, R.R., Smith, K.L., Jr. (**1985**) Live capture, maintenance and partial decompression of a deep-sea grenadier fish (*Coryphaenoides acrolepis*) in a hyperbaric trap-aquarium. *Deep-Sea Research* , Vol **32**, No 12, 1571-1582.

Yayanos, A.A. (**1978**) Recovery and maintenance of live amphipods at a pressure of 580 bars from an ocean depth of 5700 meters. *Science,* **200** (**4345**), 1056–1059. doi: 10.1126/science.200.4345.1056.

Yayanos, A.A. (**1981**) Reversible inactivation of deep-sea amphipods (Paralicella caperesca) by a decompression from 601 bars to atmospheric pressure. *Comparative Biochemistry and Physiology*, **69A**, 563-565.

Yayanos, A.A. (**2009**) Recovery of Live Amphipods at Over 102 MPa from the Challenger Deep. *Marine Technology Society Journal*, Vol **43**, Number 5, 132 – 136

FIGURES

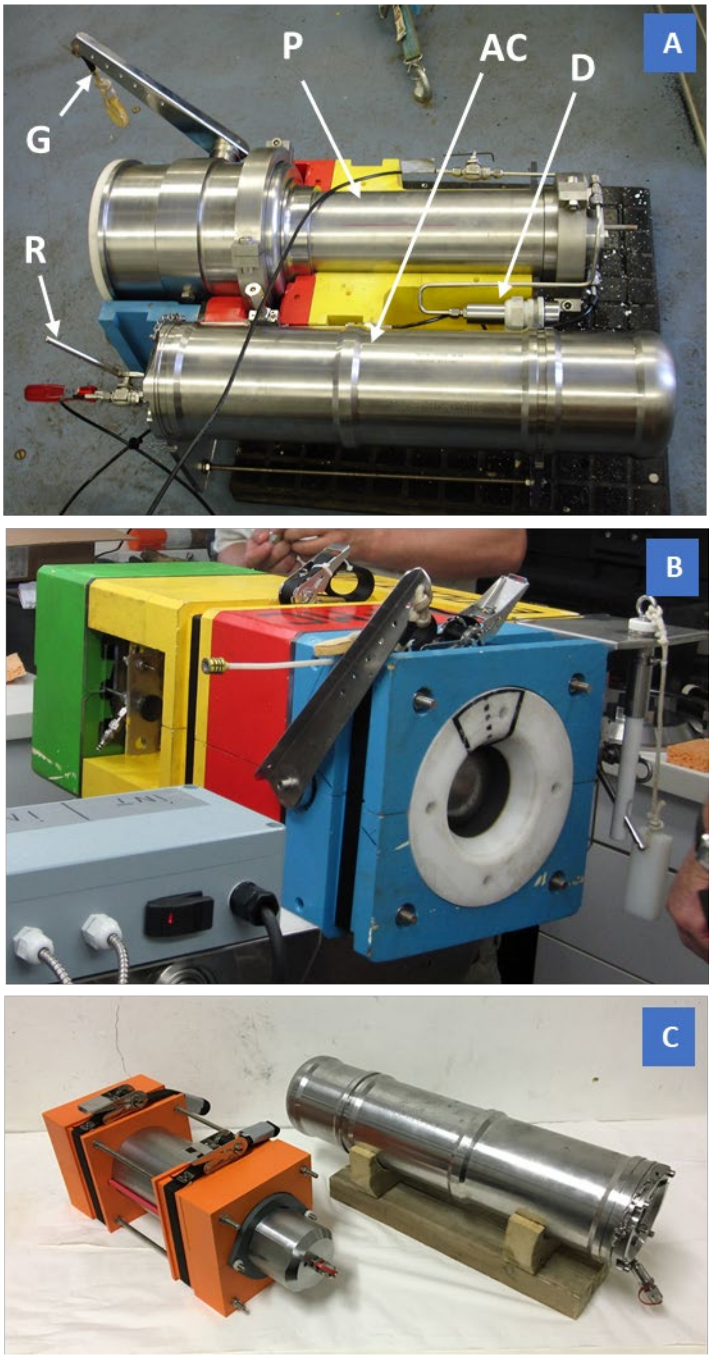

Figure 1 : The PRD PERISCOP

A, B - the PRD (P) is positioned in syntactic foam casings (here coloured in blue, red, yellow and green, fully assembled in B), with the active compensator (AC) alongside. A pressure data logger (D) is connected to the PRD. G and R are the handles of the two valves (GV and RV in figure 2) which need to be manipulated *in situ* before samples can be recovered.

C - the two types of compensators alternatively used in this work : passive (left) or active (right). Full length of the compensators are approximately 55 and 65 cm, and a diameter of 13 and 15 cm respectively.

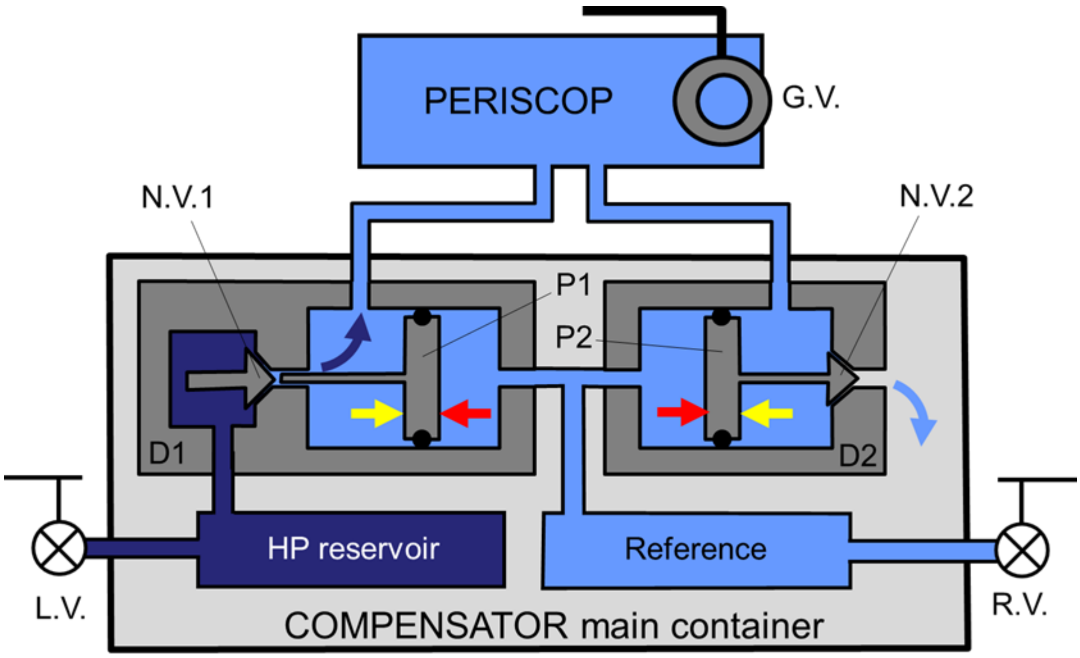

Figure 2 : Principle for active pressure compensation.
The PRD (PERISCOP) is hydraulically connected to the compensator, by means of two differential valves (also called « dome-valves ») D1 and D2 (dark grey). The compensator is composed of three containers, and two differential valves. The inside of the main container (light grey) always remains at atmospheric pressure. Inside this container, one high-pressure container (HP reservoir) is connected to D1 and to a loading valve (LV), the other one (Reference) is connected to both D1 and D2, and another valve (RV) allows connection to the surrounding environment.
Prior to sampling, HP reservoir is loaded with seawater at about 45 MPa pressure, by using LV, which further remains closed throughout the sampling operation. Upon mooring, the PRD and the reference container remain open, thus remaining at identical pressure, that of the surrounding environment. In situ, and once samples have been stored inside the PRD, its main globe-valve (GV) is closed by the submersible's hydraulic arm, before closing RV. From then on, during recovery (ascent in the water column), the reference container is not submitted to variations in surrounding pressure (because it is stored inside the main container, at atmospheric pressure). Therefore it maintains a stable internal pressure. During recovery, the pressure in the water column surrounding PRD decreases, thereby allowing expansion of the PRD walls, and consequent internal pressure loss. Therefore, the pressure inside the reference is higher (red arrows), and consequently actuates the piston (P1) and the needle-valve (NV1) of D1, resulting in extra seawater (dark blue arrow) injected from the HP reservoir towards the PRD, until pressures in PRD and Reference equilibrate. Conversely, if the pressure in PRD increases above the reference pressure (yellow arrows), the piston (P2) and needle-valve (NV2) of D2 are actuated, thereby releasing seawater inside the Compensator main container (light blue arrow), until pressures in PRD and Reference equilibrate. Note that, for clarity, the size of D1 and D2 is exaggerated on this scheme, however the water volumes enclosed in these valves is negligible compared to the volumes of PERISCOP and Reference containers.

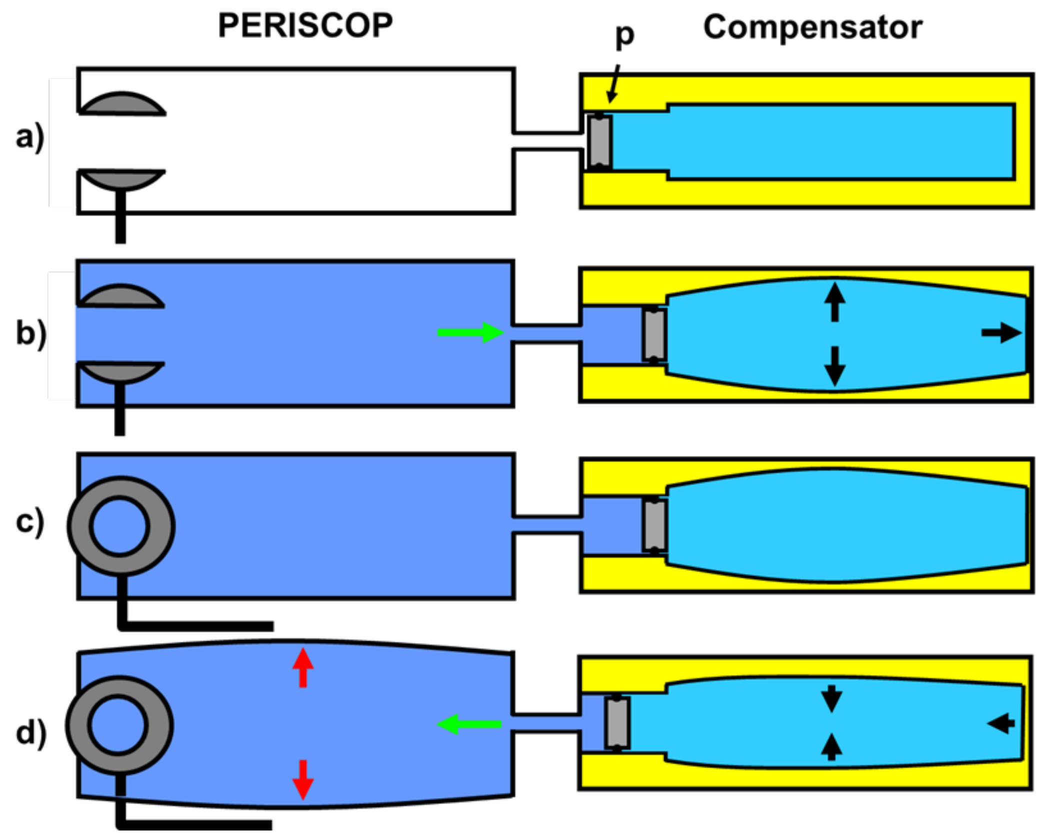

Figure 3 : Principle for passive pressure compensation.
The PRD (PERISCOP) is hydraulically connected to the compensator, by means of a piston (p). The compensator consists of a double-wall container filled with water or oil (light blue). The interspace (yellow) between container walls remains at atmospheric pressure throughout the entire sampling process.
a) Prior to mooring at depth, all compartments are at atmospheric pressure.
b) At depth, seawater (dark blue) at *in situ* pressure forces the piston back in the compensator (green arrow), thereby expanding the inner container (black arrows).
c) At depth, the globe-valve of the PRD is closed.
d) Upon recovery, the surrounding pressure decreases, thereby allowing expansion of the PRD walls (red arrows), and consequent internal pressure loss, which is partially compensated by the compensator piston forcing seawater back inside the PRD (green arrow), due to the contraction of the inner container (black arrows).

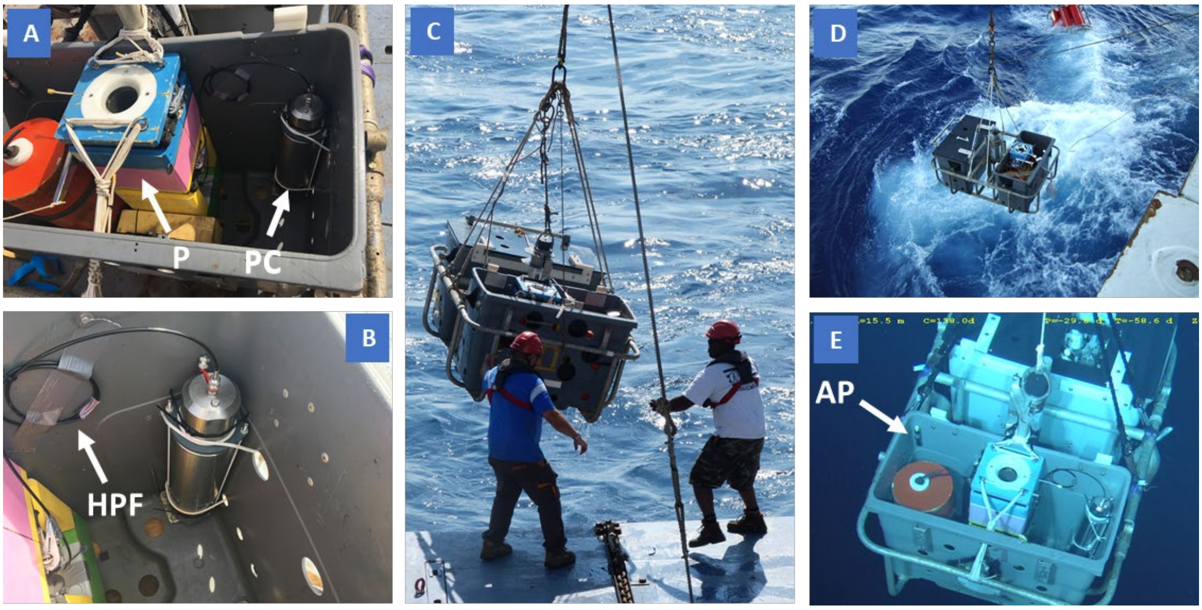

Figure 4 : Operation of the PERISCOP PRD, using a shuttle device. The shuttle presented here belongs to the Ifremer Nautile submersible team.
A : PERISCOP (P) and its passive compensator (PC) is fixed inside one of the 2 containers of the shuttle device.
B : Close-up view of the passive compensator, which is linked to the PRD through a high-pressure flexible hose (HPF).
C and D : mooring operation of the shuttle.
E : The shuttle with the PERISCOP PRD at depth (photographic credit Ifremer). An autonomous pressure/temperature probe (AP) is mounted on the shuttle's container.

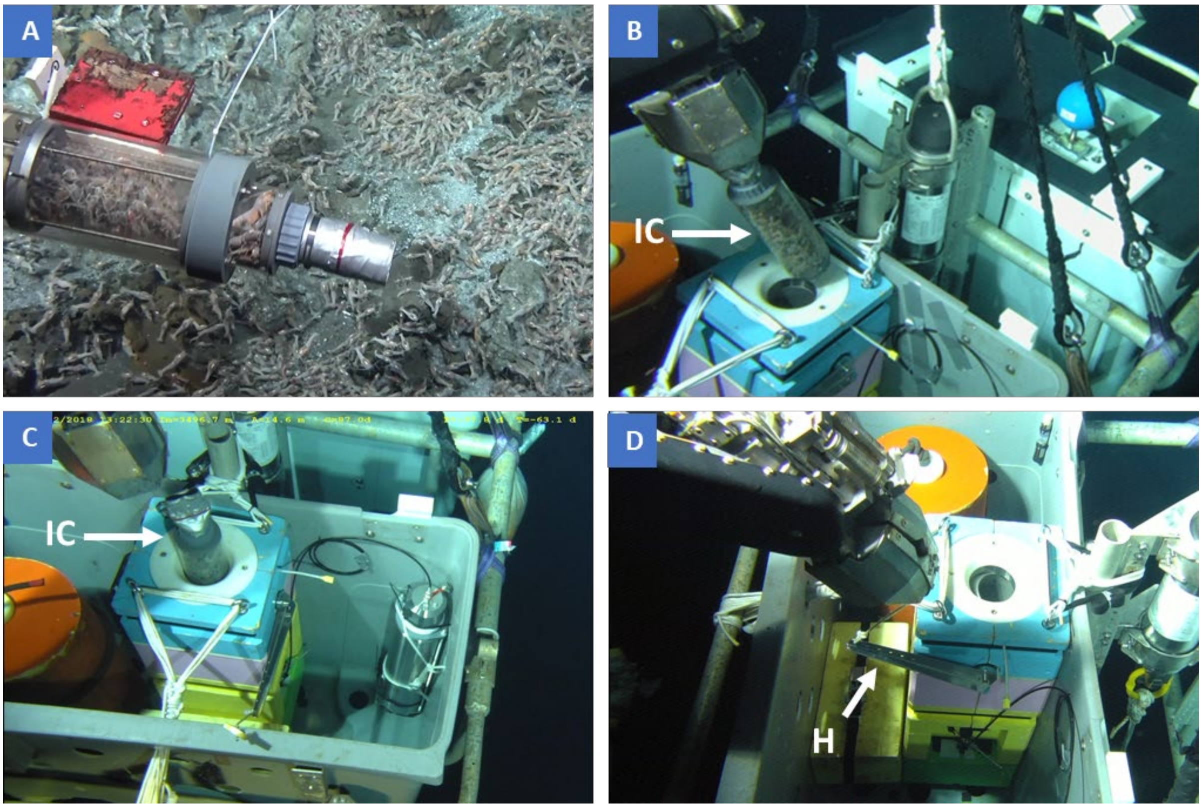

Figure 5 : *In situ* sampling with the deep-sea manned submersible Nautile at the TAG hydrothermal vent field, during the Bicose2 cruise (photographic credits Ifremer).
A : by connecting the submersible's suction device to the sampling cell (see also Shillito et al, 2008), the Nautile operators may aim for specific fauna, here vent shrimps (*Rimicaris exoculata*).
B and C : The sampling cell is disassembled, and its inner cylinder (IC) is held by the submersible's hydraulic arm, for introduction inside the PERISCOP PRD.
D : The hydraulic arm closes the PERISCOP PRD by pulling the handle (H) of the quarter-turn globe-valve.

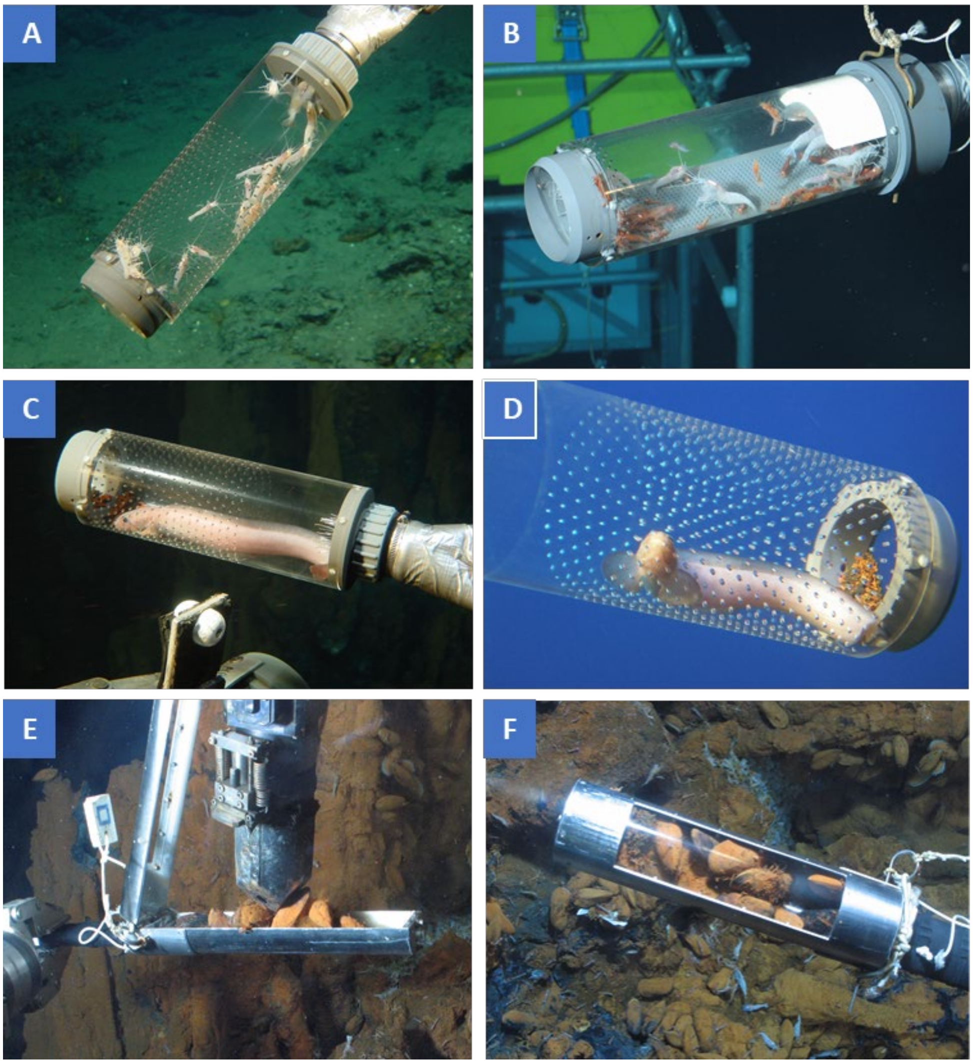

Figure 6 : Various animal samples collected with the PERISCOP PRD, on the MAR Rainbow vent field, at a depth of 2300 m (photographic credits Ifremer).
A and B : vent shrimps, *Rimicaris exoculata* and *Mirocaris fortunata.*
C and D : zoarcid fishes *Pachycara saldanhai.*
E and F : mussels, *Bathymodiolus azoricus,* collected with the Croco sampling cell.

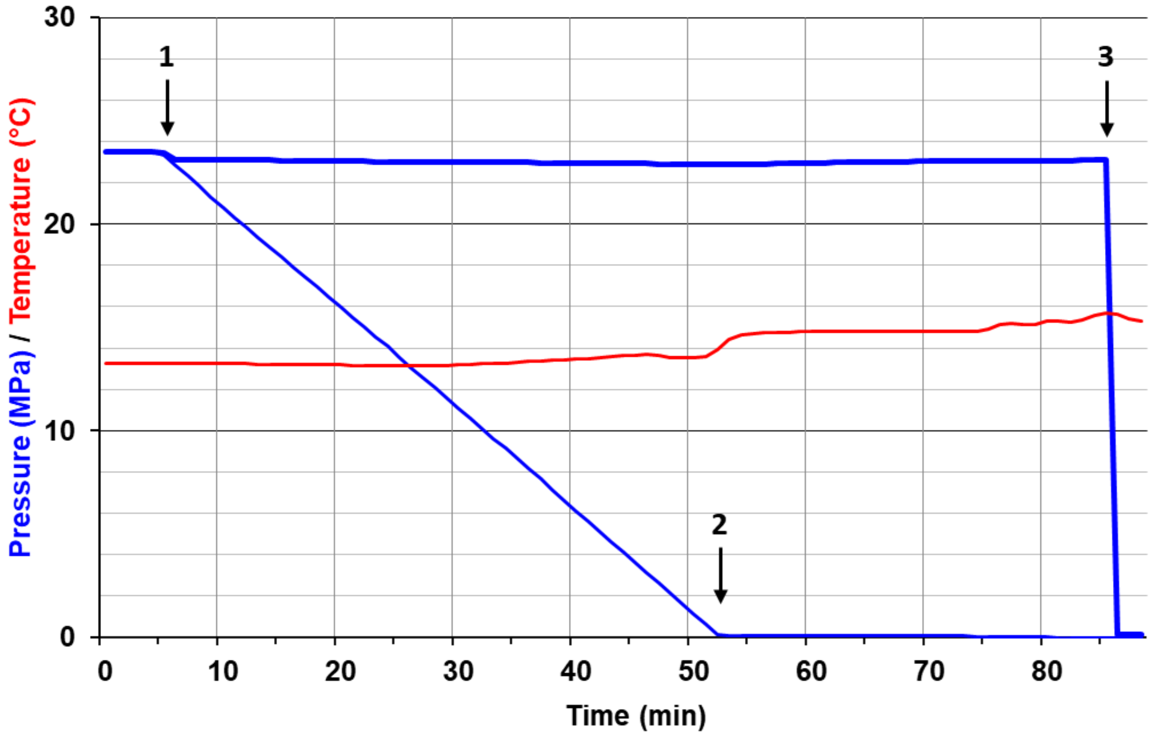

Figure 7 : Pressure (MPa) and Temperature (°C) monitoring during the recovery of the PERISCOP from about 2350 m depth in the Mediterranean Sea, using the active compensation system, as a function of time. Blue lines account for Pressure, either inside the PRD (bold line), or in the surrounding water column (thin line). The red line accounts for Temperature in the surrounding water column. Arrows indicate from 1 to 3 respectively : beginning of shuttle ascent, shuttle reaching the surface, releasing pressure of the PRD on ship deck.

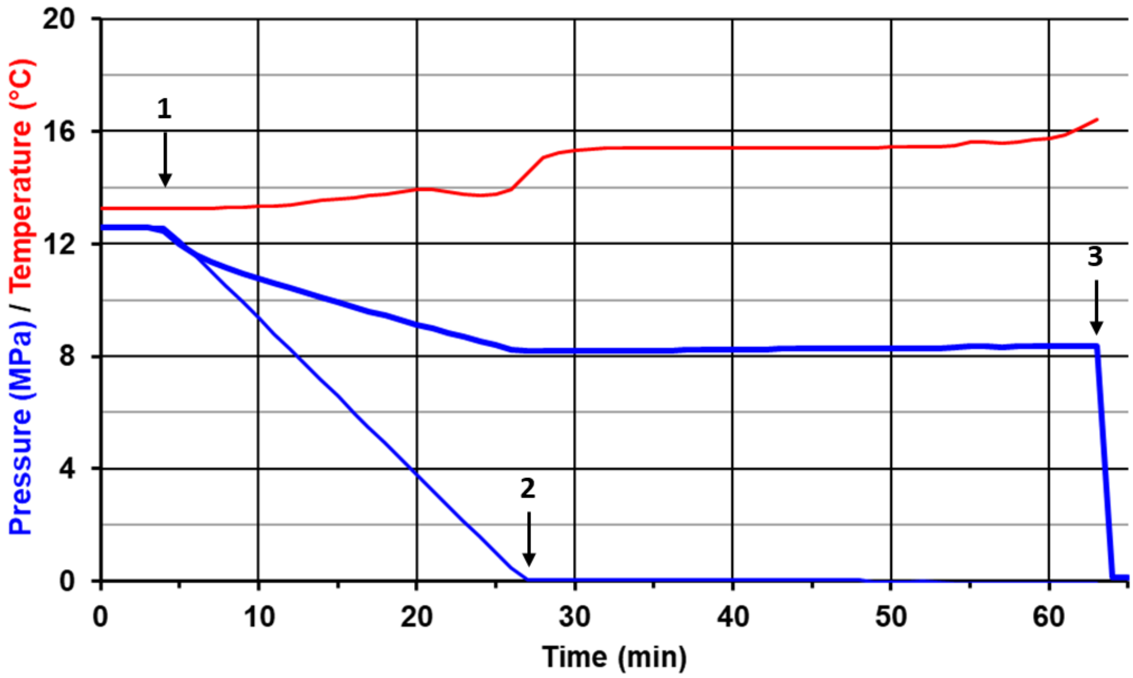

Figure 8 : Pressure (MPa) and Temperature (°C) monitoring during the recovery of the PERISCOP from about 1250 m depth in the Mediterranean Sea, with no compensation, as a function of time. Blue lines account for Pressure, either inside the PRD (bold line), or in the surrounding water column (thin line). The red line accounts for Temperature in the surrounding water column. Arrows indicate from 1 to 3 respectively : beginning of shuttle ascent, shuttle reaching the surface, releasing pressure of the PRD on ship deck.

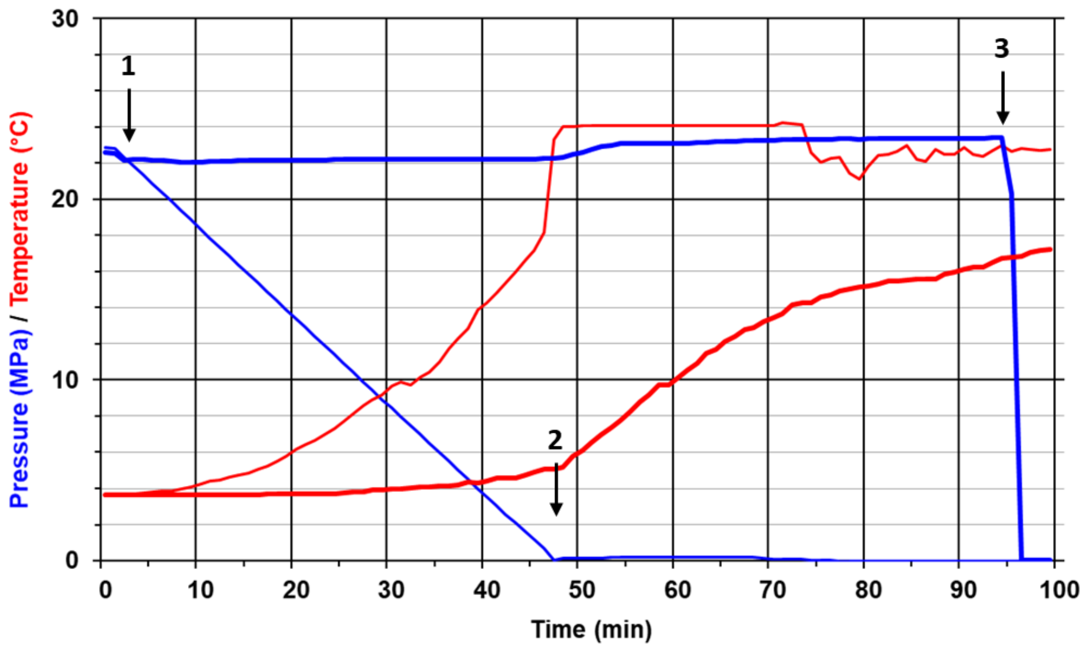

Figure 9 : Pressure (MPa) and Temperature (°C) monitoring during the recovery of the PERISCOP from about 2300 m depth at the MAR Rainbow site, using the active compensation system, as a function of time. Blue lines account for Pressure, either inside the PRD (bold line), or in the surrounding water column (thin line). Red lines account for Temperature, either inside the PRD (bold line), or in the surrounding water column (thin line). Accordingly, thick lines are recordings of pressure and temperature conditions inside the PRD, while thin lines correspond to recordings of data loggers mounted on the shuttle device which carries the PRD. Arrows indicate from 1 to 3 respectively: beginning of shuttle ascent, shuttle reaching the surface, releasing pressure of the PRD on ship deck.

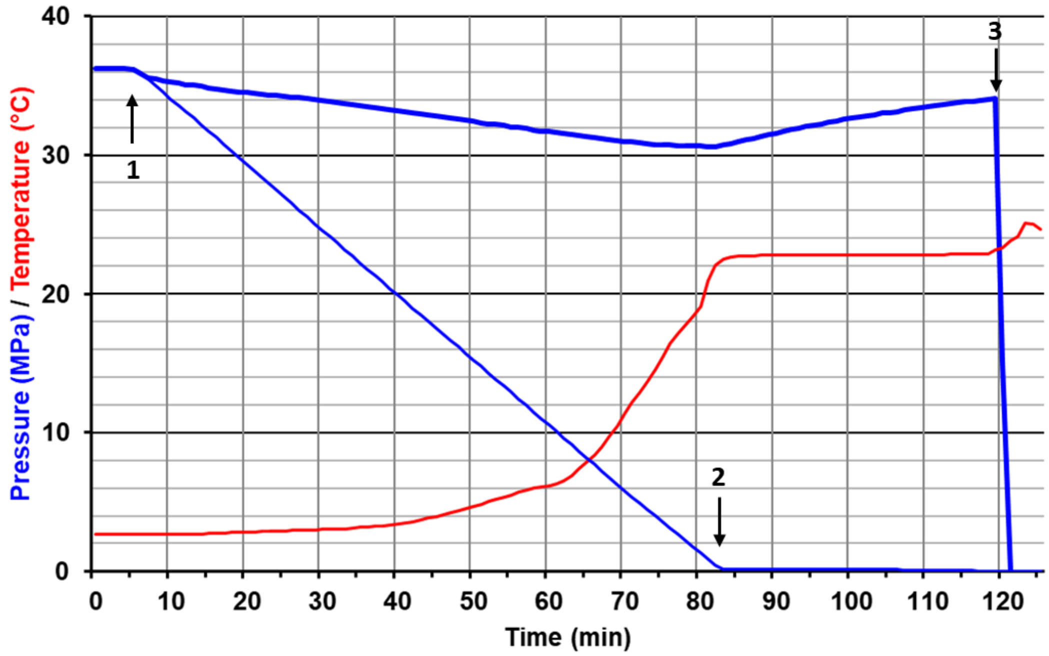

Figure 10 : Pressure (MPa) and Temperature (°C) monitoring during the recovery of the PERISCOP from about 3600 m depth at the MAR TAG site, using the passive compensation system, as a function of time. Blue lines account for Pressure, either inside the PRD (bold line), or in the surrounding water column (thin line). The Red line accounts for Temperature in the surrounding water column. Arrows indicate from 1 to 3 respectively : beginning of shuttle ascent, shuttle reaching the surface, releasing pressure of the PRD on ship deck.

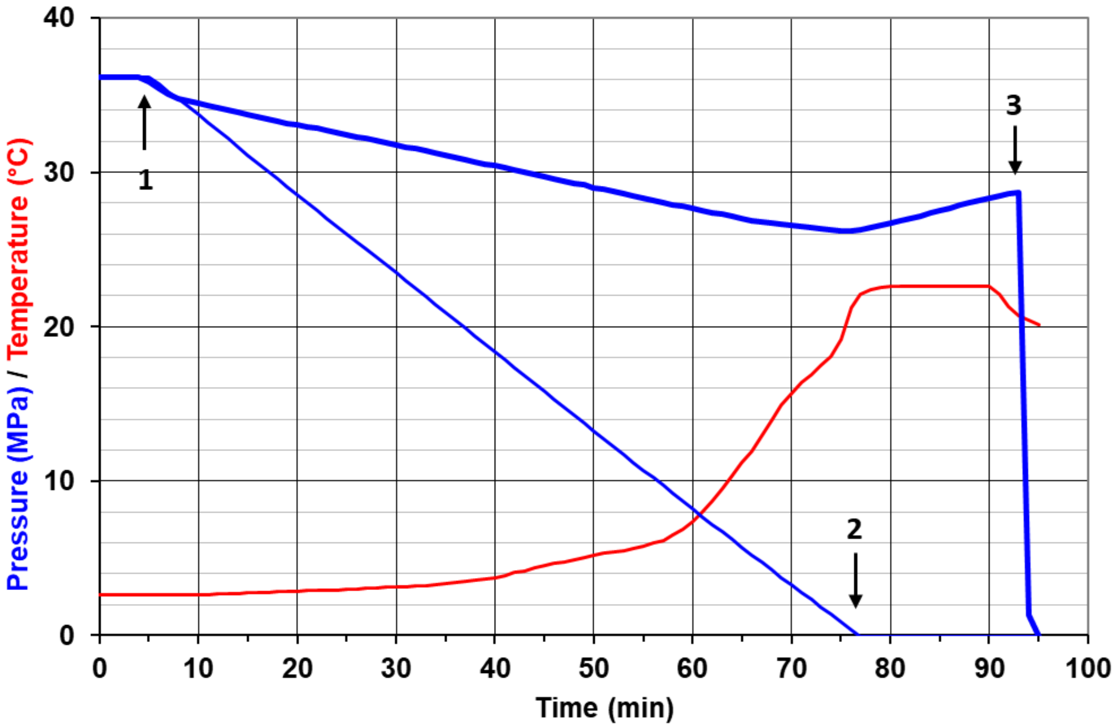

Figure 11 : Pressure (MPa) and Temperature (°C) monitoring during the recovery of the PERISCOP from about 3600 m depth at the MAR TAG site, with no compensation, as a function of time. Blue lines account for Pressure (Mpa), either inside the PRD (bold line), or in the surrounding water column (thin line). The Red line accounts for Temperature in the surrounding water column. Arrows indicate from 1 to 3 respectively : beginning of shuttle ascent, shuttle reaching the surface, shuttle being hauled out of the water, releasing pressure of the PRD on ship deck.

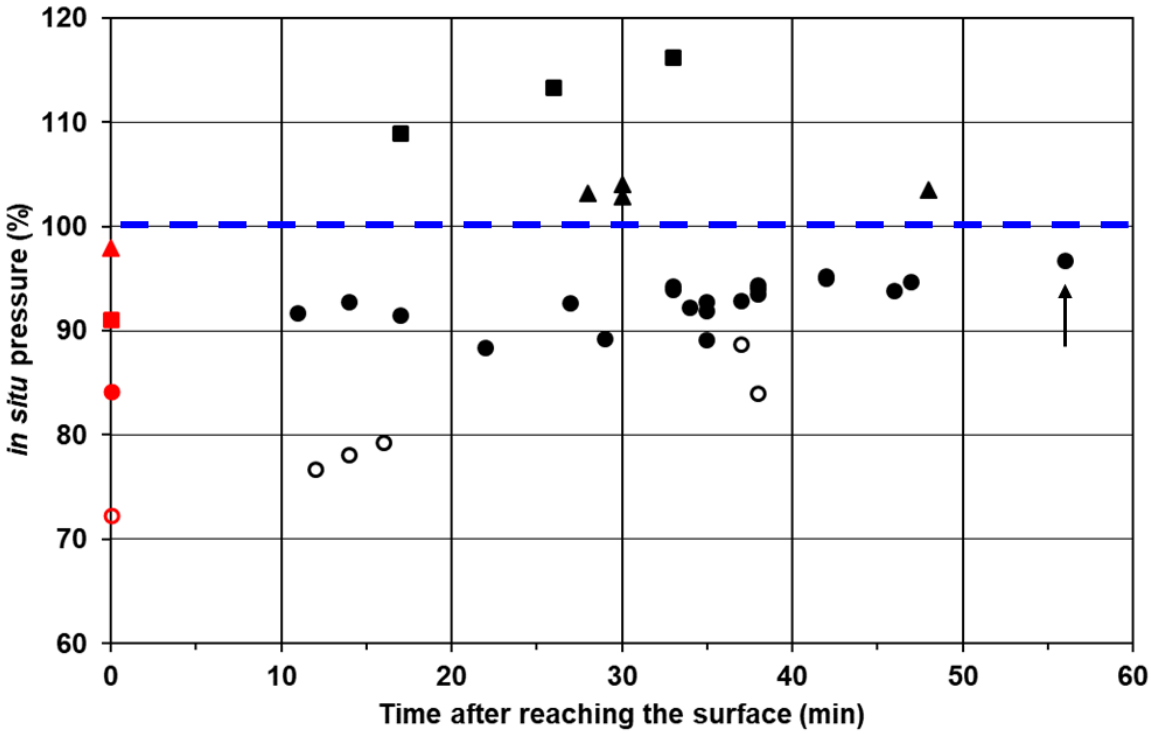

Figure 12 : Percentage of pressure retention (% of *in situ* pressure) just before releasing the pressure in the PRD, as a function of time spent in warm surface waters, for several pressurised recoveries. For example, the sampling with an arrow had a pressure of 97% of *in situ* pressure, just before pressure release and opening of the PRD on ship deck, 56 minutes after reaching the surface. All the data correspond to MAR vent fields, depths ranging from 3600 to 2300 m, with *in situ* water temperature ranging from 2.5 to 4.5 °C, and surface waters ranging from 23 to 26 °C. Empty circles : no compensation. Plain circles : water-filled passive compensation. Plain squares : oil-filled passive compensation. Plain triangles : active compensation. Red points on the vertical axis represent the mean of minimum pressure retention, which occurs upon reaching the surface (Time = 0 min).

cruise	trial #	sampling depth (m)	pressure compensation	minimum pressure (%)	final pressure (%)
EssNaut 2021	P3	1200	none	63,5	60,1
	P5	1250		65,2	66,60
	P1	2700	passive (oil)	84,1	86,7
	P2	2700		84,4	86,80
	P4	1250		83,3	89,08
EssNaut 2016	P1	2430	active	94,5	94,90
	P2	2420		95,3	96,24
	P3	1170		94,3	95,90
	P4	1180		95,3	96,26
	P5	1180		94,1	94,47
	P6	2350		97,6	98,30
	P7	2410		93,8	93,94

Table S1 : Data for several technical deployments of the PERISCOP PRD, in an isothermal column (Mediterranean Sea in winter, less than 2°C gradient between sampling site and surface water, EssNaut cruises). Pressures are given as percentage of *in situ* pressure. The deployments were undertaken either with no compensation, or oil-filled passive compensation, or active compensation.

cruise	trial #	site	sampling depth (m)	pressure compensation	minimum pressure (%)	final pressure (%)	time spent at surface (min)	comment
MomarDream	D1	Rainbow	2300	active	98,2	102,9	30	
	D2	Rainbow	2290		98,1	104,1	30	
	D4	Rainbow	2210		97,8	103,2	28	
	D5	Rainbow	2220		97,6	103,5	48	
	D3	Rainbow	2250		73,0	89,1	37	
Bicose 1	P13	TAG	3610	none	72,3	83,9	38	
	P14	TAG	3640		72,0	78,0	14	
	P15	TAG	3640		71,7	76,6	12	
	P16	TAG	3620		72,4	79,3	16	
Bicose 2	P1	TAG	3600	passive (water)	84,2	93,5	38	
	P2	TAG	3570		84,5	94,2	33	
	P3	TAG	3620		83,3	91,9	35	
	P4	TAG	3590		83,7	93,8	46	
	P5	TAG	3580		84,9	96,7	56	
	P6	TAG	3630		84,5	94,0	38	
	P7	TAG	3600		84,6	92,6	27	
	P8	TAG	3580		83,9	94,4	38	
	P9	TAG	3570		85,0	93,9	33	
	P10	TAG	3560		85,3	94,9	42	
	P11	Snake Pit	3390		84,6	95,2	42	
	P12	Snake Pit	3430		no data	no data	no data	probe failure
	P13	Snake Pit	3450		83,1	94,6	47	
	P14	Snake Pit	3440		83,1	92,2	34	
	P15	Snake Pit	3380		84,2	92,7	35	
	P16	Snake Pit	3390		84,1	92,9	37	
	P17	Snake Pit	3530		80,9	89,1	35	
	P18	Snake Pit	3480		81,4	89,2	29	
Transect	P6	Broken Spur	3100	passive (water)	83,5	88,3	22	
	P7	Broken Spur	3120		85,6	91,4	17	
	P8V	Lost City	760		71	89,2	25	leak during ascent
	P9	Broken Spur	3130		86,6	92,7	14	
	P10	Broken Spur	3090		86,4	91,7	11	
	P11	Broken Spur	3120		84,4	91,40	17	
	P1	Rainbow	2250	passive (oil)	91,1	108,9	17	
	P2V	Rainbow	2360		91,3	113,3	26	
	P3	Rainbow	2330		90,7	116,2	33	
	P4	Rainbow	2350		88,3	100	17	leak at surface
	P5V	Rainbow	2350		85,4	90,5	39	leak during ascent

Table S2 : Data for several deployments of the PERISCOP PRD, in a non-isothermal water column (MAR sites with similar temperature gradients of about 20°C between sampling site and surface water). Pressures are given as percentage of *in situ* pressure. The deployments were undertaken either with no compensation, or water-filled passive compensation, or oil-filled passive compensation.

Mean values (+/- SD) for minimum pressure (upon reaching the surface) are 72.3 +/- 0.5 for no compensation (n = 5), 84.2 +/-1.3 for water-filled compensation (n = 22), 91.0 +/- 0.3 for oil-filled compensation (n = 3), and 97.9 +/-0.3 for active compensation (n = 4). P4, P5V and P8V deployments were discarded because of leaks during ascent, or at the surface.

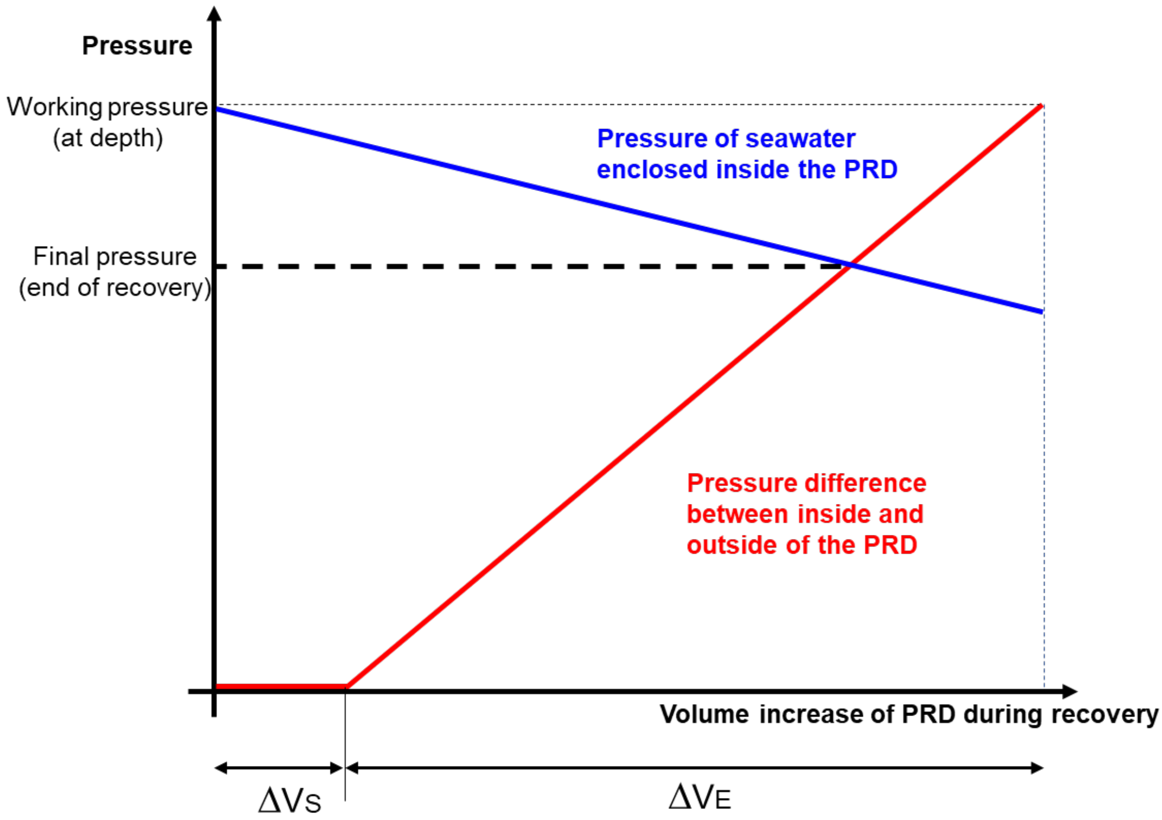

Figure S1 : Estimating the pressure-retaining performance of a PRD

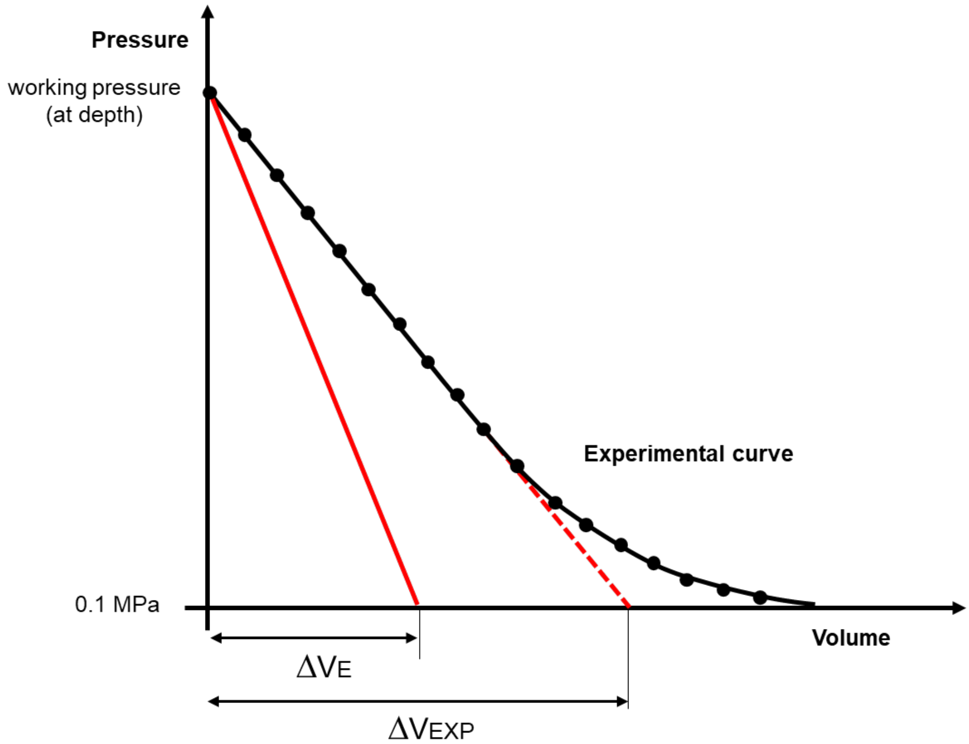

Figure S2 : Experimental determination of the expansion of PRD walls

ANNEX 1 : **Estimation of pressure-retaining capacity of the PERISCOP PRD (figures S1 and S2)**

Before choosing/designing the type of compensator needed for a PRD, it is necessary to first estimate its pressure-retaining performance, without any compensation. During PRD recovery from deep water, the surrounding hydrostatic pressure decreases due to the ascent through the water column. Consequently, a difference in pressure builds up between the water inside the PRD and the external environment (Figure S1, red curve). This difference pushes seals within their grooves, and further expands the walls of the PRD. In turn, the volume of the seawater trapped inside the PRD increases, thereby causing a drop in hydrostatic pressure (Figure S1, blue curve). The internal pressure will further decrease as long as it is higher than needed to expand the PRD walls, before reaching the final pressure, at the intercept between the two considered curves.

The expansion curve of the trapped seawater (blue curve) may be established by knowing the initial volume of the PRD, the mass of seawater trapped inside the PRD, according to pressure and temperature at depth, and the variations of seawater density as a function of pressure (McDougall and Barker, 2011). Temperature may first be considered constant throughout the process, simulating deep-sea conditions (e.g. 4°C), although it should be kept in mind that gradual heating (when approaching warm surface waters) would increase the internal pressure.

The expansion curve of the volume inside the PRD (red curve) has two contributions : seal movement and expansion of PRD walls.

Seal movement: the volume variation due to seals depends mainly on the volume displacement of seals (ΔV_S), and at lesser extent on volume change of seals while being compressed. The assumption made here is that the seawater enclosed inside the PRD expands as the external pressure is decreasing, and pushes the seals until they reach their locking position. During this process, the pressure difference between inside and outside the PRD remains small, but sufficient to push the seals.

In our study, based on the size of the seals and their maximum displacements within their respective grooves, we estimated the volume displacement to be around 3 to 5 mL. Compared to volume variations due to expansion of PRD walls (see below), this contribution of seal displacement may be considered constant, i.e. independent from pressure at which the PRD was closed.

Expansion of PRD walls: once the seals are in sealing position, the difference in pressure (inside vs. outside the PRD) builds up, therefore expanding the PRD walls. Such an expansion may be experimentally estimated (Figure S2), by repeating pressurisation/depressurisation experiments of the PRD at the laboratory. The assumption made here is that the variation in volume of the PRD when being pressurised from atmospheric pressure to working pressure at the laboratory, is similar to that experienced when the pressure surrounding the PRD decreases from working pressure to atmospheric pressure, while working pressure is maintained inside the PRD (a situation closer to operational sampling conditions). Although both final situations are identical (PRD pressurised, and surrounded by atmospheric pressure), the initial situations differ by the fact that the entire PRD (inside and outside) is either at atmospheric pressure (laboratory experiment), or at working pressure (*in situ* deployment), meaning the compressibility of steel is neglected in the laboratory experiment. Measurements of successive water volumes released from the PRD are achieved (typically in the 5-10 mL range at each sampling, for the PERISCOP PRD), upon gradual depressurisation from working pressure (pressure at which the PRD would be deployed) to atmospheric pressure. Repeated cycles allow to determine the behaviour of pressure as a function of recovered water volumes, which is almost linear, except when approaching lower pressures (below 10 MPa), due to expansion of air bubbles possibly trapped inside the PRD. Nevertheless, the linear behaviour obtained at higher pressures may be virtually extrapolated (dotted line in figure S2) in order to intercept the volume co-ordinate ΔV_{EXP} at the 0.1 MPa origin (atmospheric pressure). This volume (measured at atmospheric pressure) is converted to a volume ΔV_E, taking in account the densities of water (D_{ATM} and D_{WP}) at both atmospheric and working pressures, the temperature, and the volume of the PRD at rest (V0, or initial volume):

$$\Delta V_E = ((V0 + \Delta V_{EXP}) \times D_{ATM} / D_{WP}) - V0$$

Back to Figure S1, this will lead to a linear relation of Pressure as a function of volume, $P = k \times \Delta V + P_{ATM}$ with a slope $k = (WP - P_{ATM}) / \Delta V_E$, corresponding to the true volume variation of the PRD submitted to internal pressure, independent from the liquid experimentally employed (provided the equation of state is known, liquids other than seawater may be used).

Finally, the red curve in Figure S1 is a combination of the contribution of seals (horizontal part corresponding to ΔV_S), and the contribution of PRD wall expansion (pressure increase following the slope k, corresponding to ΔV_E). It should be noted that because ΔV_S remains constant (as opposed to ΔV_E which decreases at shallower deployment depths), this term will increasingly alter pressure retention performance as shallower deployment depths are considered.

Such an approach allowed us to estimate the expansion of the PERISCOP (ΔV_E) to be about 31 mL upon pressurisation at 30 MPa. Adding about 3-5 mL of seal movement (ΔV_S), this lead to predictions ranging from about 70% pressure retention in a simulated deployment at 3600 m depth and 4°C temperature, to about 60% for a simulated deployment at 1000 m depth.

McDougall T. J. and P. M. Barker, 2011: Getting started with TEOS-10 and the Gibbs Seawater (GSW) Oceanographic Toolbox, 28pp., SCOR/IAPSO WG127, ISBN 978-0-646--55621-5.